



ARTICLE

An Improved Interval-Valued Picture Fuzzy TOPSIS Approach Based on New Divergence Measures for Risk Assessment

Sijia Zhu¹, Yuhan Li², Prasanalakshmi Balaji^{3,*}, Akila Thiyagarajan³, Rajanikanth Aluvalu⁴ and Zhe Liu^{5,6,7,*}

¹Department of Applied Mathematics and Statistics, Johns Hopkins University, Baltimore, MD 21218, USA

²Cw Chu College, Jiangsu Normal University, Xuzhou, 221116, China

³Department of Computer Science, College of Computer Science, King Khalid University, Abha, 62521, Saudi Arabia

⁴Symbiosis Institute of Technology, Hyderabad Campus, Symbiosis International (Deemed University), Pune, 412115, India

⁵Jadara Research Center, Jadara University, Irbid, 21110, Jordan

⁶College of Mathematics and Computer, Xinyu University, Xinyu, 338004, China

⁷School of Computer Sciences, Universiti Sains Malaysia, Penang, 11800, Malaysia

*Corresponding Authors: Prasanalakshmi Balaji. Email: drsana@ieee.org; Zhe Liu. Email: liuzhe921@gmail.com

Received: 05 June 2025; Accepted: 18 July 2025; Published: 31 August 2025

ABSTRACT: While interval-valued picture fuzzy sets (IvPFSs) provide a powerful tool for modeling uncertainty and ambiguity in various fields, existing divergence measures for IvPFSs remain limited and often produce counterintuitive results. To address these shortcomings, this paper introduces two novel divergence measures for IvPFSs, inspired by the Jensen-Shannon divergence. The fundamental properties of the proposed measures—non-degeneracy, symmetry, triangular inequality, and boundedness—are rigorously proven. Comparative analyses with existing measures are conducted through specific cases and numerical examples, clearly demonstrating the advantages of our approach. Furthermore, we apply the new divergence measures to develop an enhanced interval-valued picture fuzzy TOPSIS method for risk assessment in construction projects, showing the practical applicability and effectiveness of our contributions.

KEYWORDS: Interval-valued picture fuzzy sets; divergence measure; Jensen-Shannon divergence; TOPSIS; risk assessment

1 Introduction

Uncertainty and imprecision are standard daily, especially during decision-making processes [1,2]. There has been a growing interest in recent years in how to deal with uncertainty and imprecision across multiple applications [3–5]. Over time, a wide range of classical theories has been extensively studied, for example, fuzzy set theory [6–8], Z-numbers [9], rough set theory [10], and R-numbers [11]. One significant contribution is Zadeh's [12] introduction of fuzzy sets (FSs), which have since gained widespread attention in addressing ambiguous and imprecise information. Later, researchers applied fuzzy set theory in numerous domains, including decision-making, image processing, and control systems [13–15]. Based on this, Atanassov [16] proposed intuitionistic fuzzy sets (IFSs), which integrate membership, non-membership, and hesitation degrees to handle uncertainty precisely. This approach provides a flexible framework for representing ambiguous data and has been effectively employed in areas like multi-criteria decision-making (MCDM) [17–20]. For example, to enhance ranking stability and better reflect user preferences in e-commerce decision-making, Kizielewicz et al. [21] proposed the FN-MABAC method integrates



fuzzy normalization to mitigate ranking reversals and improve alignment with reference rankings. Later, Atanassov [22] introduced interval-valued intuitionistic fuzzy sets (IvIFSs). IvIFSs use interval values for membership and non-membership, defined by their respective lower and upper bounds. This enables a flexible representation of uncertainty, making IvIFS helpful in solving various problems [23,24]. Then, Cuong and Kreinovich [25] introduced picture fuzzy sets (PFSs) to extend classical fuzzy set theory by incorporating a neutral membership degree alongside positive and negative memberships, thereby enabling a better representation of uncertainty or indecision. PFSs, with their four degrees-positive, negative, neutral, and refusal-are particularly useful in decision-making scenarios that involve ambiguity, such as medical diagnostics and personnel evaluations [26–29].

Although PFSs improve the ability to manage uncertainty, they still depend on exact membership values. This can be a limitation in complex situations where uncertainty changes or the information is unclear. Therefore, Cuong and Kreinovich [30] introduced interval-valued picture fuzzy sets (IvPFSs), a significant development of PFSs. IvPFSs address the limitations of fixed membership degrees in the original PFS framework. It represents positive, negative, neutral, and refusal membership degrees as intervals instead of single values, offering a more flexible and comprehensive approach. This adjustment considers the natural variability and uncertainty in real-world decisions. The interval values in IvPFSs make it easier to model uncertainty more accurately, especially in applications like risk assessment, medical diagnosis, and construction decision-making, where data are often not exact and range within specific ranges [31,32]. Researchers [33–36] have developed various measures to enhance the applicability of IvPFSs. Khalil et al. [37] introduced novel operations and addressed related decision-making challenges. Ma et al. [38] combined IvPFS with an MCDM process to effectively evaluate design concepts under uncertainty, using an integrated approach with entropy weighting and an extended TOPSIS method.

The exploration of divergence measures has played a crucial role in developing fuzzy sets and has drawn extensive interest [39,40]. Many researchers have developed measures for IFSs and PFSs. For instance, Hatzimichilidis et al. [41] introduced matrix norms and fuzzy implications for IFSs. Jiang et al. [42] proposed an IFS distance method and validated its effectiveness through clustering. Wu et al. [43] proposed an important intuitionistic fuzzy distance measure based on Jensen-Shannon (JS) divergence, enhancing the ability to distinguish and rank IFSs. Singh et al. [44] developed a range of distance measures on PFSs with adjustable parameters, including the normalized Hamming, Euclidean, and Hausdorff distances. Yuan et al. [45] introduced a JS divergence-based distance measure for PFSs with a maximum deviation approach for alternative ranking. Zhu et al. [46] introduced two distance measures on PFSs based on JS divergence. However, these works did not extend the fuzzy numbers to interval values. Thus, several distance or divergence measures have been specifically created for IvIFSs and IvPFSs. Xu and Chen [47] provided enhanced IvIFSs with weighted and geometric distance models. Gohain et al. [48] proposed an optimistic distance measure for IvIFSs with cross-time information and applied it to clustering tasks in engineering problems. Mishra et al. [49] introduced a novel divergence measure for IvIFSs and proposed a vehicle insurance solution. Zhu and Liu [50] developed novel distance metrics for PFSs and IvPFSs using Hellinger distance and showed superior performance. Khan et al. [51] combined IvPFSs and hypergraphs to evaluate their role in enhancing processes. While these methods have demonstrated differing degrees of effectiveness, some limitations remain:

- There is a significant gap in divergence measures for IvPFSs, with limited research and scarce literature available on this topic.
- Several existing distance measures for IvPFSs fail to satisfy the basic axioms.
- Certain established measures produce inconsistent or unforeseen outcomes when evaluating the differences between diverse IvPFSs.

The work presents two novel measures for IvPFSs, intending to resolve the limitations of existing methods and the significant gap for IvPFSs. The key contributions can be summarized in four aspects:

- We propose two new JS divergence measures for IvPFSs.
- We prove that the introduced measures satisfy the fundamental principles that define divergence measures.
- We introduce divergence measures that can efficiently solve and correct the counterintuitive results observed in some instances with existing measures.
- We propose an improved interval-valued picture fuzzy TOPSIS approach based on new divergence measures for risk assessment in construction projects.

The structure of this manuscript is illustrated in Fig. 1. Section 2 gives the fundamental concepts. In Section 3, two novel distance measures based on Jensen-Shannon divergence for IvPFSs are introduced with comprehensive proofs and derivations. Section 4 conducts various numerical analyses to assess proposed measures in comparison to existing ones, using diverse case studies. Section 5 implements the TOPSIS method within the context of a construction risk assessment challenge, culminating in significant findings and recommendations for future research in risk evaluation. Finally, Section 6 provides the conclusions and prospective future work.

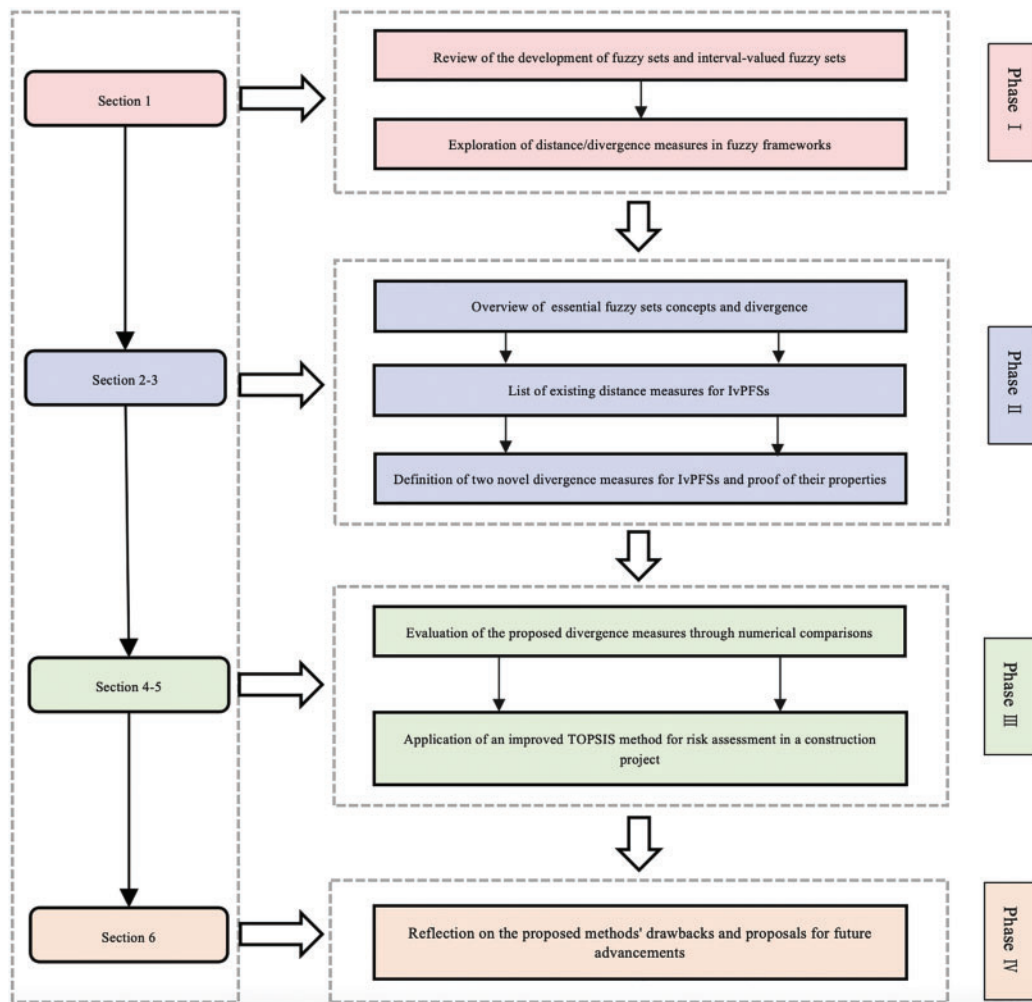


Figure 1: The flow chart of the whole work

2 Preliminaries

This section will present some essential concepts and review several existing distance measures.

2.1 Basic Concepts of Fuzzy Sets

Definition 1 ([12]). Consider a universe of discourse (UOD) $Y = \{o_1, o_2, \dots, o_n\}$. A fuzzy set (FS) is described as follows:

$$\mathfrak{J} = \{o, \xi_{\mathfrak{J}}(o) \mid o \in Y\} \quad (1)$$

where $\xi_{\mathfrak{J}}(o) \in [0, 1]$ expresses the membership. For each $o \in Y$, we have $0 \leq \xi_{\mathfrak{J}}(o) \leq 1$ and $\varsigma_{\mathfrak{J}}(o) = 1 - \xi_{\mathfrak{J}}(o)$, and $\varsigma_{\mathfrak{J}}(o) : o \rightarrow [0, 1]$ indicates the non-membership related to $o \in Y$.

Definition 2 ([16]). An intuitionistic fuzzy set (IFS) in Y is defined as follows:

$$\mathfrak{J} = \{o, \xi_{\mathfrak{J}}(o), \varsigma_{\mathfrak{J}}(o) \mid o \in Y\} \quad (2)$$

where $\xi_{\mathfrak{J}}(o), \varsigma_{\mathfrak{J}}(o) : o \rightarrow [0, 1]$ express the membership and non-membership. For each $o \in Y$, we have $\xi_{\mathfrak{J}}(o) + \varsigma_{\mathfrak{J}}(o) \leq 1$ and $\zeta_{\mathfrak{J}}(o) = 1 - \xi_{\mathfrak{J}}(o) - \varsigma_{\mathfrak{J}}(o)$, where $\zeta_{\mathfrak{J}}(o) : o \rightarrow [0, 1]$ reveals the hesitancy degree of $o \in Y$.

Definition 3 ([22]). An interval-valued intuitionistic fuzzy set (IvIFS) in X is defined as follows:

$$\mathfrak{J} = \{o, \xi_{\mathfrak{J}}(o), \varsigma_{\mathfrak{J}}(o) \mid o \in Y\} \quad (3)$$

where $\xi_{\mathfrak{J}}(o) = [\xi_{\mathfrak{J}}^L(o), \xi_{\mathfrak{J}}^U(o)]$ and $\varsigma_{\mathfrak{J}}(o) = [\varsigma_{\mathfrak{J}}^L(o), \varsigma_{\mathfrak{J}}^U(o)]$. These intervals indicate the extent to which an element exhibits positive and negative membership in a set. For $\forall o \in Y$, we have $\xi_{\mathfrak{J}}(o) + \varsigma_{\mathfrak{J}}(o) \leq 1$ and $\zeta_{\mathfrak{J}}(o) = 1 - \xi_{\mathfrak{J}}(o) - \varsigma_{\mathfrak{J}}(o)$, where $\zeta_{\mathfrak{J}}(o) = [\zeta_{\mathfrak{J}}^L(o), \zeta_{\mathfrak{J}}^U(o)]$ indicates neutral membership within the ranges of $o \in Y$.

Definition 4 ([25]). A picture fuzzy set (PFS) in X is defined as follows:

$$\mathfrak{J} = \{o, \xi_{\mathfrak{J}}(o), \varsigma_{\mathfrak{J}}(o), \zeta_{\mathfrak{J}}(o) \mid o \in Y\} \quad (4)$$

where $\xi_{\mathfrak{J}}(o), \varsigma_{\mathfrak{J}}(o), \zeta_{\mathfrak{J}}(o) \in [0, 1]$ express positive membership, negative membership, and neutral membership degrees. For each $o \in Y$, we have $\xi_{\mathfrak{J}}(o) + \varsigma_{\mathfrak{J}}(o) + \zeta_{\mathfrak{J}}(o) \leq 1$ and $\omega_{\mathfrak{J}}(o) = 1 - \xi_{\mathfrak{J}}(o) - \varsigma_{\mathfrak{J}}(o) - \zeta_{\mathfrak{J}}(o)$, where $\omega_{\mathfrak{J}}(o) : o \rightarrow [0, 1]$ represents refusal membership degree of $o \in Y$.

Definition 5 ([30]). An interval-valued picture fuzzy set (IvPFS) in X is defined as follows:

$$\mathfrak{J} = \{o, \xi_{\mathfrak{J}}(o), \varsigma_{\mathfrak{J}}(o), \zeta_{\mathfrak{J}}(o) \mid o \in Y\} \quad (5)$$

where $\xi_{\mathfrak{J}}(o) = [\xi_{\mathfrak{J}}^L(o), \xi_{\mathfrak{J}}^U(o)]$, $\varsigma_{\mathfrak{J}}(o) = [\varsigma_{\mathfrak{J}}^L(o), \varsigma_{\mathfrak{J}}^U(o)]$ and $\zeta_{\mathfrak{J}}(o) = [\zeta_{\mathfrak{J}}^L(o), \zeta_{\mathfrak{J}}^U(o)]$. These intervals represent the degrees of positive, negative, and neutral membership that an element holds. For all $o \in Y$, we have $\xi_{\mathfrak{J}}(o) + \varsigma_{\mathfrak{J}}(o) + \zeta_{\mathfrak{J}}(o) \leq 1$ and $\omega_{\mathfrak{J}}(o) = 1 - \xi_{\mathfrak{J}}(o) - \varsigma_{\mathfrak{J}}(o) - \zeta_{\mathfrak{J}}(o)$, where $\omega_{\mathfrak{J}}(o) : o \rightarrow [0, 1]$, where $\omega_{\mathfrak{J}}(o) = [\omega_{\mathfrak{J}}^L(o), \omega_{\mathfrak{J}}^U(o)]$ indicates refusal membership within the ranges of $o \in Y$.

2.2 The Existing Distance Measures for IvPFSs

To showcase the advantages of the distance measure proposed in this paper, this subsection will first present current distance measures in Table 1 and compare them with the proposed measure, highlighting their limitations in Section 4.

Table 1: Existing distance measures of IvPFSs

Ref.	Distance measures
Liu et al. [52]	$\mathbb{D}_L^1(\mathfrak{J} \mathfrak{H}) = 1 - \frac{1}{n} \sum_{i=1}^n \cos \left\{ \frac{\pi}{2} \left[\begin{array}{l} \xi_{\mathfrak{J}}^L(\mathfrak{o}_i) - \xi_{\mathfrak{H}}^L(\mathfrak{o}_i) \vee \xi_{\mathfrak{J}}^R(h_i) - \xi_{\mathfrak{H}}^R(\mathfrak{o}_i) \\ \vee \zeta_{\mathfrak{J}}^L(\mathfrak{o}_i) - \zeta_{\mathfrak{H}}^L(\mathfrak{o}_i) \vee \zeta_{\mathfrak{J}}^R(\mathfrak{o}_i) - \zeta_{\mathfrak{H}}^R(\mathfrak{o}_i) \\ \vee \zeta_{\mathfrak{J}}^L(\mathfrak{o}_i) - \zeta_{\mathfrak{H}}^L(\mathfrak{o}_i) \vee \zeta_{\mathfrak{J}}^R(\mathfrak{o}_i) - \zeta_{\mathfrak{H}}^R(\mathfrak{o}_i) \end{array} \right] \right\}$
Liu et al. [52]	$\mathbb{D}_L^2(\mathfrak{J} \mathfrak{H}) = 1 - \frac{1}{n} \sum_{i=1}^n \cos \left\{ \frac{\pi}{4} \left[\begin{array}{l} \xi_{\mathfrak{J}}^L(\mathfrak{o}_i) - \xi_{\mathfrak{H}}^L(\mathfrak{o}_i) + \xi_{\mathfrak{J}}^R(h_i) - \xi_{\mathfrak{H}}^R(\mathfrak{o}_i) \\ + \zeta_{\mathfrak{J}}^L(\mathfrak{o}_i) - \zeta_{\mathfrak{H}}^L(\mathfrak{o}_i) + \zeta_{\mathfrak{J}}^R(\mathfrak{o}_i) - \zeta_{\mathfrak{H}}^R(\mathfrak{o}_i) \\ + \zeta_{\mathfrak{J}}^L(\mathfrak{o}_i) - \zeta_{\mathfrak{H}}^L(\mathfrak{o}_i) + \zeta_{\mathfrak{J}}^R(\mathfrak{o}_i) - \zeta_{\mathfrak{H}}^R(\mathfrak{o}_i) \end{array} \right] \right\}$
Cao and Shen [53]	$\mathbb{D}_{CS}^1(\mathfrak{J} \mathfrak{H}) = \sqrt{\frac{1}{64n} \sum_{i=1}^n \left(\begin{array}{l} \left[\begin{array}{l} 3(\xi_{\mathfrak{J}}^L(\mathfrak{o}_i) - \xi_{\mathfrak{H}}^L(\mathfrak{o}_i))^2 \\ - (\zeta_{\mathfrak{J}}^L(\mathfrak{o}_i) - \zeta_{\mathfrak{H}}^L(\mathfrak{o}_i))^2 \\ - (\zeta_{\mathfrak{J}}^R(\mathfrak{o}_i) - \zeta_{\mathfrak{H}}^R(\mathfrak{o}_i))^2 \end{array} \right] + \left[\begin{array}{l} 3(\xi_{\mathfrak{J}}^R(\mathfrak{o}_i) - \xi_{\mathfrak{H}}^R(\mathfrak{o}_i))^2 \\ - (\zeta_{\mathfrak{J}}^R(\mathfrak{o}_i) - \zeta_{\mathfrak{H}}^R(\mathfrak{o}_i))^2 \\ - (\zeta_{\mathfrak{J}}^L(\mathfrak{o}_i) - \zeta_{\mathfrak{H}}^L(\mathfrak{o}_i))^2 \end{array} \right] \\ + \left[\begin{array}{l} 3(\xi_{\mathfrak{J}}^L(\mathfrak{o}_i) - \xi_{\mathfrak{H}}^L(\mathfrak{o}_i))^2 \\ - (\zeta_{\mathfrak{J}}^L(\mathfrak{o}_i) - \zeta_{\mathfrak{H}}^L(\mathfrak{o}_i))^2 \\ - (\zeta_{\mathfrak{J}}^R(\mathfrak{o}_i) - \zeta_{\mathfrak{H}}^R(\mathfrak{o}_i))^2 \end{array} \right] + \left[\begin{array}{l} 3(\xi_{\mathfrak{J}}^R(\mathfrak{o}_i) - \xi_{\mathfrak{H}}^R(\mathfrak{o}_i))^2 \\ - (\zeta_{\mathfrak{J}}^R(\mathfrak{o}_i) - \zeta_{\mathfrak{H}}^R(\mathfrak{o}_i))^2 \\ - (\zeta_{\mathfrak{J}}^L(\mathfrak{o}_i) - \zeta_{\mathfrak{H}}^L(\mathfrak{o}_i))^2 \end{array} \right] \end{array} \right)}$
Cao and Shen [53]	$\mathbb{D}_{CS}^2(\mathfrak{J} \mathfrak{H}) = \sqrt{\frac{1}{100n} \sum_{i=1}^n \left(\begin{array}{l} \left[\begin{array}{l} 4(\xi_{\mathfrak{J}}^L(\mathfrak{o}_i) - \xi_{\mathfrak{H}}^L(\mathfrak{o}_i))^2 \\ - (\zeta_{\mathfrak{J}}^L(\mathfrak{o}_i) - \zeta_{\mathfrak{H}}^L(\mathfrak{o}_i))^2 \\ - (\zeta_{\mathfrak{J}}^R(\mathfrak{o}_i) - \zeta_{\mathfrak{H}}^R(\mathfrak{o}_i))^2 \end{array} \right] + \left[\begin{array}{l} 4(\xi_{\mathfrak{J}}^R(\mathfrak{o}_i) - \xi_{\mathfrak{H}}^R(\mathfrak{o}_i))^2 \\ - (\zeta_{\mathfrak{J}}^R(\mathfrak{o}_i) - \zeta_{\mathfrak{H}}^R(\mathfrak{o}_i))^2 \\ - (\zeta_{\mathfrak{J}}^L(\mathfrak{o}_i) - \zeta_{\mathfrak{H}}^L(\mathfrak{o}_i))^2 \end{array} \right] \\ + \left[\begin{array}{l} 4(\xi_{\mathfrak{J}}^L(\mathfrak{o}_i) - \xi_{\mathfrak{H}}^L(\mathfrak{o}_i))^2 \\ - (\zeta_{\mathfrak{J}}^L(\mathfrak{o}_i) - \zeta_{\mathfrak{H}}^L(\mathfrak{o}_i))^2 \\ - (\zeta_{\mathfrak{J}}^R(\mathfrak{o}_i) - \zeta_{\mathfrak{H}}^R(\mathfrak{o}_i))^2 \end{array} \right] + \left[\begin{array}{l} 4(\xi_{\mathfrak{J}}^R(\mathfrak{o}_i) - \xi_{\mathfrak{H}}^R(\mathfrak{o}_i))^2 \\ - (\zeta_{\mathfrak{J}}^R(\mathfrak{o}_i) - \zeta_{\mathfrak{H}}^R(\mathfrak{o}_i))^2 \\ - (\zeta_{\mathfrak{J}}^L(\mathfrak{o}_i) - \zeta_{\mathfrak{H}}^L(\mathfrak{o}_i))^2 \end{array} \right] \end{array} \right)}$
Zhu et al. [50]	$\mathbb{D}_Z^1(\mathfrak{J}, \mathfrak{H}) = \frac{1}{2n} \sum_{i=1}^n \max \left(\begin{array}{l} \sqrt{\xi_{\mathfrak{J}}^L(\mathfrak{o}_i)} - \sqrt{\xi_{\mathfrak{H}}^L(\mathfrak{o}_i)} , \sqrt{\xi_{\mathfrak{J}}^U(\mathfrak{o}_i)} - \sqrt{\xi_{\mathfrak{H}}^U(\mathfrak{o}_i)} \\ \sqrt{\zeta_{\mathfrak{J}}^L(\mathfrak{o}_i)} - \sqrt{\zeta_{\mathfrak{H}}^L(\mathfrak{o}_i)} , \sqrt{\zeta_{\mathfrak{J}}^U(\mathfrak{o}_i)} - \sqrt{\zeta_{\mathfrak{H}}^U(\mathfrak{o}_i)} \\ \sqrt{\omega_{\mathfrak{J}}^L(\mathfrak{o}_i)} - \sqrt{\omega_{\mathfrak{H}}^L(\mathfrak{o}_i)} , \sqrt{\omega_{\mathfrak{J}}^U(\mathfrak{o}_i)} - \sqrt{\omega_{\mathfrak{H}}^U(\mathfrak{o}_i)} \end{array} \right)$
Zhu et al. [50]	$\mathbb{D}_Z^2(\mathfrak{J}, \mathfrak{H}) = \frac{1}{2n} \sum_{i=1}^n \max \left(\begin{array}{l} \sqrt{\xi_{\mathfrak{J}}^L(\mathfrak{o}_i)} - \sqrt{\xi_{\mathfrak{H}}^L(\mathfrak{o}_i)} ^2, \sqrt{\xi_{\mathfrak{J}}^U(\mathfrak{o}_i)} - \sqrt{\xi_{\mathfrak{H}}^U(\mathfrak{o}_i)} ^2 \\ \sqrt{\zeta_{\mathfrak{J}}^L(\mathfrak{o}_i)} - \sqrt{\zeta_{\mathfrak{H}}^L(\mathfrak{o}_i)} ^2, \sqrt{\zeta_{\mathfrak{J}}^U(\mathfrak{o}_i)} - \sqrt{\zeta_{\mathfrak{H}}^U(\mathfrak{o}_i)} ^2 \\ \sqrt{\omega_{\mathfrak{J}}^L(\mathfrak{o}_i)} - \sqrt{\omega_{\mathfrak{H}}^L(\mathfrak{o}_i)} ^2, \sqrt{\omega_{\mathfrak{J}}^U(\mathfrak{o}_i)} - \sqrt{\omega_{\mathfrak{H}}^U(\mathfrak{o}_i)} ^2 \end{array} \right)$

2.3 Jensen-Shannon Divergence

The Jensen-Shannon (JS) divergence finds extensive applications in areas such as machine learning and information theory for comparing different probability distributions.

Definition 6. Let \mathbf{P} and \mathbf{Q} denote two probability distributions, represented as $\mathbf{P} = \{p_1, p_2, \dots, p_m\}$ and $\mathbf{Q} = \{q_1, q_2, \dots, q_m\}$. The JS divergence can be mathematically expressed as follows:

$$JS(\mathbf{P}, \mathbf{Q}) = H\left(\frac{\mathbf{P} + \mathbf{Q}}{2}\right) - \frac{1}{2}H(\mathbf{P}) - \frac{1}{2}H(\mathbf{Q})$$

$$= \frac{1}{2} \left[\sum_j p_j \log \left(\frac{2p_j}{p_j + q_j} \right) + \sum_j q_j \log \left(\frac{2q_j}{p_j + q_j} \right) \right] \quad (6)$$

where the entropy $H(\mathbf{P}) = -\sum_{j=1}^m p_j \log p_j$ and $H(\mathbf{Q}) = -\sum_{j=1}^m q_j \log q_j$, with logarithm taken to base 2.

3 New Divergence Measure for IvPFSs

This section presents two new divergence measures for IvPFSs from the Jensen-Shannon divergence.

Definition 7. Let $\mathfrak{D} = \{\mathfrak{o}_1, \mathfrak{o}_2, \dots, \mathfrak{o}_n\}$ be a UOD. For two IvPFSs $\mathfrak{J} = \{\langle \xi_{\mathfrak{J}}(\mathfrak{o}), \varsigma_{\mathfrak{J}}(\mathfrak{o}), \zeta_{\mathfrak{J}}(\mathfrak{o}) \rangle | \mathfrak{o} \in Y\}$ where $\xi_{\mathfrak{J}}(\mathfrak{o}) = [\xi_{\mathfrak{J}}^L(\mathfrak{o}), \xi_{\mathfrak{J}}^U(\mathfrak{o})]$, $\varsigma_{\mathfrak{J}}(\mathfrak{o}) = [\varsigma_{\mathfrak{J}}^L(\mathfrak{o}), \varsigma_{\mathfrak{J}}^U(\mathfrak{o})]$ and $\zeta_{\mathfrak{J}}(\mathfrak{o}) = [\zeta_{\mathfrak{J}}^L(\mathfrak{o}), \zeta_{\mathfrak{J}}^U(\mathfrak{o})]$, similarly $\xi_{\mathfrak{H}}(\mathfrak{o})$, $\varsigma_{\mathfrak{H}}(\mathfrak{o})$ and $\zeta_{\mathfrak{H}}(\mathfrak{o})$ correspond to \mathfrak{H} . Subsequently, a JS divergence, denoted as $JS_{IvPFS}^1(\mathfrak{J}, \mathfrak{H})$, for the IvPFSs \mathfrak{J} and \mathfrak{H} can be expressed by the following equation:

$$JS_{IvPFS}^1(\mathfrak{J}, \mathfrak{H}) = \frac{1}{4} \left(\begin{aligned} & \xi_{\mathfrak{J}}^L(\mathfrak{o}_i) \log \frac{2\xi_{\mathfrak{J}}^L(\mathfrak{o}_i)}{\xi_{\mathfrak{J}}^L(\mathfrak{o}_i) + \xi_{\mathfrak{H}}^L(\mathfrak{o}_i)} + \xi_{\mathfrak{J}}^U(\mathfrak{o}_i) \log \frac{2\xi_{\mathfrak{J}}^U(\mathfrak{o}_i)}{\xi_{\mathfrak{J}}^U(\mathfrak{o}_i) + \xi_{\mathfrak{H}}^U(\mathfrak{o}_i)} \\ & + \xi_{\mathfrak{H}}^L(\mathfrak{o}_i) \log \frac{2\xi_{\mathfrak{H}}^L(\mathfrak{o}_i)}{\xi_{\mathfrak{J}}^L(\mathfrak{o}_i) + \xi_{\mathfrak{H}}^L(\mathfrak{o}_i)} + \xi_{\mathfrak{H}}^U(\mathfrak{o}_i) \log \frac{2\xi_{\mathfrak{H}}^U(\mathfrak{o}_i)}{\xi_{\mathfrak{J}}^U(\mathfrak{o}_i) + \xi_{\mathfrak{H}}^U(\mathfrak{o}_i)} \\ & + \varsigma_{\mathfrak{J}}^L(\mathfrak{o}_i) \log \frac{2\varsigma_{\mathfrak{J}}^L(\mathfrak{o}_i)}{\varsigma_{\mathfrak{J}}^L(\mathfrak{o}_i) + \varsigma_{\mathfrak{H}}^L(\mathfrak{o}_i)} + \varsigma_{\mathfrak{J}}^U(\mathfrak{o}_i) \log \frac{2\varsigma_{\mathfrak{J}}^U(\mathfrak{o}_i)}{\varsigma_{\mathfrak{J}}^U(\mathfrak{o}_i) + \varsigma_{\mathfrak{H}}^U(\mathfrak{o}_i)} \\ & + \varsigma_{\mathfrak{H}}^L(\mathfrak{o}_i) \log \frac{2\varsigma_{\mathfrak{H}}^L(\mathfrak{o}_i)}{\varsigma_{\mathfrak{J}}^L(\mathfrak{o}_i) + \varsigma_{\mathfrak{H}}^L(\mathfrak{o}_i)} + \varsigma_{\mathfrak{H}}^U(\mathfrak{o}_i) \log \frac{2\varsigma_{\mathfrak{H}}^U(\mathfrak{o}_i)}{\varsigma_{\mathfrak{J}}^U(\mathfrak{o}_i) + \varsigma_{\mathfrak{H}}^U(\mathfrak{o}_i)} \\ & + \zeta_{\mathfrak{J}}^L(\mathfrak{o}_i) \log \frac{2\zeta_{\mathfrak{J}}^L(\mathfrak{o}_i)}{\zeta_{\mathfrak{J}}^L(\mathfrak{o}_i) + \zeta_{\mathfrak{H}}^L(\mathfrak{o}_i)} + \zeta_{\mathfrak{J}}^U(\mathfrak{o}_i) \log \frac{2\zeta_{\mathfrak{J}}^U(\mathfrak{o}_i)}{\zeta_{\mathfrak{J}}^U(\mathfrak{o}_i) + \zeta_{\mathfrak{H}}^U(\mathfrak{o}_i)} \\ & + \zeta_{\mathfrak{H}}^L(\mathfrak{o}_i) \log \frac{2\zeta_{\mathfrak{H}}^L(\mathfrak{o}_i)}{\zeta_{\mathfrak{J}}^L(\mathfrak{o}_i) + \zeta_{\mathfrak{H}}^L(\mathfrak{o}_i)} + \zeta_{\mathfrak{H}}^U(\mathfrak{o}_i) \log \frac{2\zeta_{\mathfrak{H}}^U(\mathfrak{o}_i)}{\zeta_{\mathfrak{J}}^U(\mathfrak{o}_i) + \zeta_{\mathfrak{H}}^U(\mathfrak{o}_i)} \end{aligned} \right) \quad (7)$$

Definition 8. Assume \mathfrak{D} is a UOD. For two IvPFSs $\mathfrak{J} = \{\langle \xi_{\mathfrak{J}}(\mathfrak{o}), \varsigma_{\mathfrak{J}}(\mathfrak{o}), \zeta_{\mathfrak{J}}(\mathfrak{o}) \rangle | \mathfrak{o} \in Y\}$ where $\xi_{\mathfrak{J}}(\mathfrak{o}) = [\xi_{\mathfrak{J}}^L(\mathfrak{o}), \xi_{\mathfrak{J}}^U(\mathfrak{o})]$, $\varsigma_{\mathfrak{J}}(\mathfrak{o}) = [\varsigma_{\mathfrak{J}}^L(\mathfrak{o}), \varsigma_{\mathfrak{J}}^U(\mathfrak{o})]$ and $\zeta_{\mathfrak{J}}(\mathfrak{o}) = [\zeta_{\mathfrak{J}}^L(\mathfrak{o}), \zeta_{\mathfrak{J}}^U(\mathfrak{o})]$, similarly $\xi_{\mathfrak{H}}(\mathfrak{o})$, $\varsigma_{\mathfrak{H}}(\mathfrak{o})$ and $\zeta_{\mathfrak{H}}(\mathfrak{o})$ correspond to \mathfrak{H} . Let $\omega_{\mathfrak{J}}(\mathfrak{o})$ and $\omega_{\mathfrak{H}}(\mathfrak{o})$ denote the rejection levels of x with respect to \mathfrak{J} and \mathfrak{H} respectively. The other JS divergence, known as $JS_{IvPFS}^2(\mathfrak{J}, \mathfrak{H})$ for the IvPFSs \mathfrak{J} and \mathfrak{H} is defined as:

$$JS_{IvPFS}^2(\mathfrak{J}, \mathfrak{H}) = \frac{1}{4} \left(\begin{aligned} & \xi_{\mathfrak{J}}^L(\mathfrak{o}_i) \log \frac{2\xi_{\mathfrak{J}}^L(\mathfrak{o}_i)}{\xi_{\mathfrak{J}}^L(\mathfrak{o}_i) + \xi_{\mathfrak{H}}^L(\mathfrak{o}_i)} + \xi_{\mathfrak{J}}^U(\mathfrak{o}_i) \log \frac{2\xi_{\mathfrak{J}}^U(\mathfrak{o}_i)}{\xi_{\mathfrak{J}}^U(\mathfrak{o}_i) + \xi_{\mathfrak{H}}^U(\mathfrak{o}_i)} \\ & + \xi_{\mathfrak{H}}^L(\mathfrak{o}_i) \log \frac{2\xi_{\mathfrak{H}}^L(\mathfrak{o}_i)}{\xi_{\mathfrak{J}}^L(\mathfrak{o}_i) + \xi_{\mathfrak{H}}^L(\mathfrak{o}_i)} + \xi_{\mathfrak{H}}^U(\mathfrak{o}_i) \log \frac{2\xi_{\mathfrak{H}}^U(\mathfrak{o}_i)}{\xi_{\mathfrak{J}}^U(\mathfrak{o}_i) + \xi_{\mathfrak{H}}^U(\mathfrak{o}_i)} \\ & + \varsigma_{\mathfrak{J}}^L(\mathfrak{o}_i) \log \frac{2\varsigma_{\mathfrak{J}}^L(\mathfrak{o}_i)}{\varsigma_{\mathfrak{J}}^L(\mathfrak{o}_i) + \varsigma_{\mathfrak{H}}^L(\mathfrak{o}_i)} + \varsigma_{\mathfrak{J}}^U(\mathfrak{o}_i) \log \frac{2\varsigma_{\mathfrak{J}}^U(\mathfrak{o}_i)}{\varsigma_{\mathfrak{J}}^U(\mathfrak{o}_i) + \varsigma_{\mathfrak{H}}^U(\mathfrak{o}_i)} \\ & + \varsigma_{\mathfrak{H}}^L(\mathfrak{o}_i) \log \frac{2\varsigma_{\mathfrak{H}}^L(\mathfrak{o}_i)}{\varsigma_{\mathfrak{J}}^L(\mathfrak{o}_i) + \varsigma_{\mathfrak{H}}^L(\mathfrak{o}_i)} + \varsigma_{\mathfrak{H}}^U(\mathfrak{o}_i) \log \frac{2\varsigma_{\mathfrak{H}}^U(\mathfrak{o}_i)}{\varsigma_{\mathfrak{J}}^U(\mathfrak{o}_i) + \varsigma_{\mathfrak{H}}^U(\mathfrak{o}_i)} \\ & + \zeta_{\mathfrak{J}}^L(\mathfrak{o}_i) \log \frac{2\zeta_{\mathfrak{J}}^L(\mathfrak{o}_i)}{\zeta_{\mathfrak{J}}^L(\mathfrak{o}_i) + \zeta_{\mathfrak{H}}^L(\mathfrak{o}_i)} + \zeta_{\mathfrak{J}}^U(\mathfrak{o}_i) \log \frac{2\zeta_{\mathfrak{J}}^U(\mathfrak{o}_i)}{\zeta_{\mathfrak{J}}^U(\mathfrak{o}_i) + \zeta_{\mathfrak{H}}^U(\mathfrak{o}_i)} \\ & + \zeta_{\mathfrak{H}}^L(\mathfrak{o}_i) \log \frac{2\zeta_{\mathfrak{H}}^L(\mathfrak{o}_i)}{\zeta_{\mathfrak{J}}^L(\mathfrak{o}_i) + \zeta_{\mathfrak{H}}^L(\mathfrak{o}_i)} + \zeta_{\mathfrak{H}}^U(\mathfrak{o}_i) \log \frac{2\zeta_{\mathfrak{H}}^U(\mathfrak{o}_i)}{\zeta_{\mathfrak{J}}^U(\mathfrak{o}_i) + \zeta_{\mathfrak{H}}^U(\mathfrak{o}_i)} \\ & + \omega_{\mathfrak{J}}^L(\mathfrak{o}_i) \log \frac{2\omega_{\mathfrak{J}}^L(\mathfrak{o}_i)}{\omega_{\mathfrak{J}}^L(\mathfrak{o}_i) + \omega_{\mathfrak{H}}^L(\mathfrak{o}_i)} + \omega_{\mathfrak{J}}^U(\mathfrak{o}_i) \log \frac{2\omega_{\mathfrak{J}}^U(\mathfrak{o}_i)}{\omega_{\mathfrak{J}}^U(\mathfrak{o}_i) + \omega_{\mathfrak{H}}^U(\mathfrak{o}_i)} \\ & + \omega_{\mathfrak{H}}^L(\mathfrak{o}_i) \log \frac{2\omega_{\mathfrak{H}}^L(\mathfrak{o}_i)}{\omega_{\mathfrak{J}}^L(\mathfrak{o}_i) + \omega_{\mathfrak{H}}^L(\mathfrak{o}_i)} + \omega_{\mathfrak{H}}^U(\mathfrak{o}_i) \log \frac{2\omega_{\mathfrak{H}}^U(\mathfrak{o}_i)}{\omega_{\mathfrak{J}}^U(\mathfrak{o}_i) + \omega_{\mathfrak{H}}^U(\mathfrak{o}_i)} \end{aligned} \right) \quad (8)$$

Definition 9. The normalized distance based on the Jensen-Shannon divergence between IvPFSs \mathfrak{J} and \mathfrak{H} is represented as $\mathbb{D}_{IvPFS}^1(\mathfrak{J}, \mathfrak{H})$ for three dimensions in Eq. (9). In comparison, for four dimensions it is expressed as $\mathbb{D}_{IvPFS}^2(\mathfrak{J}, \mathfrak{H})$ in Eq. (10).

$$\begin{aligned} \mathbb{D}_{IvPFS}^1(\mathfrak{J}, \mathfrak{H}) &= \frac{1}{n} \sum_{i=1}^n \sqrt{JS_{IvPFS}^1(\mathfrak{J}, \mathfrak{H})} \\ &= \frac{1}{n} \sum_{i=1}^n \sqrt{\frac{1}{4} \left(\begin{aligned} &\xi_{\mathfrak{J}}^L(o_i) \log \frac{2\xi_{\mathfrak{J}}^L(o_i)}{\xi_{\mathfrak{J}}^L(o_i) + \xi_{\mathfrak{H}}^L(o_i)} + \xi_{\mathfrak{J}}^U(o_i) \log \frac{2\xi_{\mathfrak{J}}^U(o_i)}{\xi_{\mathfrak{J}}^U(o_i) + \xi_{\mathfrak{H}}^U(o_i)} \\ &+ \xi_{\mathfrak{H}}^L(o_i) \log \frac{2\xi_{\mathfrak{H}}^L(o_i)}{\xi_{\mathfrak{J}}^L(o_i) + \xi_{\mathfrak{H}}^L(o_i)} + \xi_{\mathfrak{H}}^U(o_i) \log \frac{2\xi_{\mathfrak{H}}^U(o_i)}{\xi_{\mathfrak{J}}^U(o_i) + \xi_{\mathfrak{H}}^U(o_i)} \\ &+ \varsigma_{\mathfrak{J}}^L(o_i) \log \frac{2\varsigma_{\mathfrak{J}}^L(o_i)}{\varsigma_{\mathfrak{J}}^L(o_i) + \varsigma_{\mathfrak{H}}^L(o_i)} + \varsigma_{\mathfrak{J}}^U(o_i) \log \frac{2\varsigma_{\mathfrak{J}}^U(o_i)}{\varsigma_{\mathfrak{J}}^U(o_i) + \varsigma_{\mathfrak{H}}^U(o_i)} \\ &+ \varsigma_{\mathfrak{H}}^L(o_i) \log \frac{2\varsigma_{\mathfrak{H}}^L(o_i)}{\varsigma_{\mathfrak{J}}^L(o_i) + \varsigma_{\mathfrak{H}}^L(o_i)} + \varsigma_{\mathfrak{H}}^U(o_i) \log \frac{2\varsigma_{\mathfrak{H}}^U(o_i)}{\varsigma_{\mathfrak{J}}^U(o_i) + \varsigma_{\mathfrak{H}}^U(o_i)} \\ &+ \zeta_{\mathfrak{J}}^L(o_i) \log \frac{2\zeta_{\mathfrak{J}}^L(o_i)}{\zeta_{\mathfrak{J}}^L(o_i) + \zeta_{\mathfrak{H}}^L(o_i)} + \zeta_{\mathfrak{J}}^U(o_i) \log \frac{2\zeta_{\mathfrak{J}}^U(o_i)}{\zeta_{\mathfrak{J}}^U(o_i) + \zeta_{\mathfrak{H}}^U(o_i)} \\ &+ \zeta_{\mathfrak{H}}^L(o_i) \log \frac{2\zeta_{\mathfrak{H}}^L(o_i)}{\zeta_{\mathfrak{J}}^L(o_i) + \zeta_{\mathfrak{H}}^L(o_i)} + \zeta_{\mathfrak{H}}^U(o_i) \log \frac{2\zeta_{\mathfrak{H}}^U(o_i)}{\zeta_{\mathfrak{J}}^U(o_i) + \zeta_{\mathfrak{H}}^U(o_i)} \end{aligned} \right)} \end{aligned} \quad (9)$$

$$\begin{aligned} \mathbb{D}_{IvPFS}^2(\mathfrak{J}, \mathfrak{H}) &= \frac{1}{n} \sum_{i=1}^n \sqrt{JS_{IvPFS}^2(\mathfrak{J}, \mathfrak{H})} \\ &= \frac{1}{n} \sum_{i=1}^n \sqrt{\frac{1}{4} \left(\begin{aligned} &\xi_{\mathfrak{J}}^L(o_i) \log \frac{2\xi_{\mathfrak{J}}^L(o_i)}{\xi_{\mathfrak{J}}^L(o_i) + \xi_{\mathfrak{H}}^L(o_i)} + \xi_{\mathfrak{J}}^U(o_i) \log \frac{2\xi_{\mathfrak{J}}^U(o_i)}{\xi_{\mathfrak{J}}^U(o_i) + \xi_{\mathfrak{H}}^U(o_i)} \\ &+ \xi_{\mathfrak{H}}^L(o_i) \log \frac{2\xi_{\mathfrak{H}}^L(o_i)}{\xi_{\mathfrak{J}}^L(o_i) + \xi_{\mathfrak{H}}^L(o_i)} + \xi_{\mathfrak{H}}^U(o_i) \log \frac{2\xi_{\mathfrak{H}}^U(o_i)}{\xi_{\mathfrak{J}}^U(o_i) + \xi_{\mathfrak{H}}^U(o_i)} \\ &+ \varsigma_{\mathfrak{J}}^L(o_i) \log \frac{2\varsigma_{\mathfrak{J}}^L(o_i)}{\varsigma_{\mathfrak{J}}^L(o_i) + \varsigma_{\mathfrak{H}}^L(o_i)} + \varsigma_{\mathfrak{J}}^U(o_i) \log \frac{2\varsigma_{\mathfrak{J}}^U(o_i)}{\varsigma_{\mathfrak{J}}^U(o_i) + \varsigma_{\mathfrak{H}}^U(o_i)} \\ &+ \varsigma_{\mathfrak{H}}^L(o_i) \log \frac{2\varsigma_{\mathfrak{H}}^L(o_i)}{\varsigma_{\mathfrak{J}}^L(o_i) + \varsigma_{\mathfrak{H}}^L(o_i)} + \varsigma_{\mathfrak{H}}^U(o_i) \log \frac{2\varsigma_{\mathfrak{H}}^U(o_i)}{\varsigma_{\mathfrak{J}}^U(o_i) + \varsigma_{\mathfrak{H}}^U(o_i)} \\ &+ \zeta_{\mathfrak{J}}^L(o_i) \log \frac{2\zeta_{\mathfrak{J}}^L(o_i)}{\zeta_{\mathfrak{J}}^L(o_i) + \zeta_{\mathfrak{H}}^L(o_i)} + \zeta_{\mathfrak{J}}^U(o_i) \log \frac{2\zeta_{\mathfrak{J}}^U(o_i)}{\zeta_{\mathfrak{J}}^U(o_i) + \zeta_{\mathfrak{H}}^U(o_i)} \\ &+ \zeta_{\mathfrak{H}}^L(o_i) \log \frac{2\zeta_{\mathfrak{H}}^L(o_i)}{\zeta_{\mathfrak{J}}^L(o_i) + \zeta_{\mathfrak{H}}^L(o_i)} + \zeta_{\mathfrak{H}}^U(o_i) \log \frac{2\zeta_{\mathfrak{H}}^U(o_i)}{\zeta_{\mathfrak{J}}^U(o_i) + \zeta_{\mathfrak{H}}^U(o_i)} \\ &+ \omega_{\mathfrak{J}}^L(o_i) \log \frac{2\omega_{\mathfrak{J}}^L(o_i)}{\omega_{\mathfrak{J}}^L(o_i) + \omega_{\mathfrak{H}}^L(o_i)} + \omega_{\mathfrak{J}}^U(o_i) \log \frac{2\omega_{\mathfrak{J}}^U(o_i)}{\omega_{\mathfrak{J}}^U(o_i) + \omega_{\mathfrak{H}}^U(o_i)} \\ &+ \omega_{\mathfrak{H}}^L(o_i) \log \frac{2\omega_{\mathfrak{H}}^L(o_i)}{\omega_{\mathfrak{J}}^L(o_i) + \omega_{\mathfrak{H}}^L(o_i)} + \omega_{\mathfrak{H}}^U(o_i) \log \frac{2\omega_{\mathfrak{H}}^U(o_i)}{\omega_{\mathfrak{J}}^U(o_i) + \omega_{\mathfrak{H}}^U(o_i)} \end{aligned} \right)} \end{aligned} \quad (10)$$

Specifically, we define that when $\xi_{\mathfrak{J}}(o) = \xi_{\mathfrak{H}}(o) = [0, 0]$, $\log \frac{1}{\xi_{\mathfrak{J}}^L(o_i) + \xi_{\mathfrak{H}}^L(o_i)} = 0$, the same with $\xi_{\mathfrak{H}}^U(o_i)$, $\xi_{\mathfrak{J}}^U(o_i)$, $\varsigma_{\mathfrak{J}}(o_i)$, $\zeta_{\mathfrak{J}}(o_i)$, $\omega_{\mathfrak{J}}(o_i)$ can be similarly defined as in the previous definition.

Remark: The divergence values from our proposed Jensen-Shannon-based measures for IvPFSs possess interpretable informational significance. Specifically, the JS divergence quantifies the dissimilarity between two IvPFSs by evaluating the average information gain when one distribution is used to approximate another. For IvPFSs, this means that the divergence score reflects the cumulative uncertainty difference across all interval-valued membership components (i.e., positive, negative, neutral, and refusal).

A divergence value close to 0 indicates that the two IvPFSs exhibit highly similar uncertainty structures. In contrast, values closer to 1 imply substantial differences in their interval-based representations of membership and hesitation. Geometrically, these measures correspond to the “distance” between interval-valued vectors in a normalized probabilistic space, accounting for both the position and spread of the intervals.

Property 1. Let \mathfrak{J} , \mathfrak{H} and \mathcal{O} be three IvPFSs in UOD X . Then $\mathbb{D}_{IvPFS}(\mathfrak{J}, \mathfrak{H})$ has the following properties:

1. $\mathbb{D}_{IvPFS}(\mathfrak{J}, \mathfrak{H}) = 0$ if and only if $\mathfrak{J} = \mathfrak{H}$.

2. $\tilde{\mathbb{D}}_{IvPFS}(\mathfrak{J}, \mathfrak{H}) = \tilde{\mathbb{D}}_{IvPFS}(\mathfrak{H}, \mathfrak{J}).$
3. $\tilde{\mathbb{D}}_{IvPFS}(\mathfrak{J}, \mathfrak{H}) + \tilde{\mathbb{D}}_{IvPFS}(\mathfrak{H}, \mathcal{O}) \geq \tilde{\mathbb{D}}_{IvPFS}(\mathfrak{J}, \mathcal{O}).$
4. $0 \leq \tilde{\mathbb{D}}_{IvPFS}(\mathfrak{J}, \mathfrak{H}) \leq 1.$

We illustrate the validity of the above axiom by taking $\tilde{\mathbb{D}}_{IvPFS}^1(\mathfrak{J}, \mathfrak{H})$ as an example.

Proof: Given $\mathfrak{J} = \mathfrak{H}$, we acquire

$$\begin{aligned}\xi_{\mathfrak{J}}^L(o_i) &= \xi_{\mathfrak{H}}^L(o_i), \xi_{\mathfrak{J}}^U(o_i) = \xi_{\mathfrak{H}}^U(o_i), \\ \varsigma_{\mathfrak{J}}^L(o_i) &= \varsigma_{\mathfrak{H}}^L(o_i), \varsigma_{\mathfrak{J}}^U(o_i) = \varsigma_{\mathfrak{H}}^U(o_i), \\ \zeta_{\mathfrak{J}}^L(o_i) &= \zeta_{\mathfrak{H}}^L(o_i), \zeta_{\mathfrak{J}}^U(o_i) = \zeta_{\mathfrak{H}}^U(o_i).\end{aligned}$$

Then, we can obtain

$$\begin{aligned}\log \frac{2\xi_{\mathfrak{J}}^L(o_i)}{\xi_{\mathfrak{J}}^L(o_i) + \xi_{\mathfrak{H}}^L(o_i)} &= \log \frac{2\xi_{\mathfrak{J}}^U(o_i)}{\xi_{\mathfrak{J}}^U(o_i) + \xi_{\mathfrak{H}}^U(o_i)}, \\ \log \frac{2\varsigma_{\mathfrak{J}}^L(o_i)}{\varsigma_{\mathfrak{J}}^L(o_i) + \varsigma_{\mathfrak{H}}^L(o_i)} &= \log \frac{2\varsigma_{\mathfrak{J}}^U(o_i)}{\varsigma_{\mathfrak{J}}^U(o_i) + \varsigma_{\mathfrak{H}}^U(o_i)}, \\ \log \frac{2\zeta_{\mathfrak{J}}^L(o_i)}{\zeta_{\mathfrak{J}}^L(o_i) + \zeta_{\mathfrak{H}}^L(o_i)} &= \log \frac{2\zeta_{\mathfrak{J}}^U(o_i)}{\zeta_{\mathfrak{J}}^U(o_i) + \zeta_{\mathfrak{H}}^U(o_i)}.\end{aligned}$$

Likewise, if $\tilde{\mathbb{D}}_{IvPFS}^1(\mathfrak{J}, \mathfrak{H}) = 0$, we can get

$$\begin{aligned}\xi_{\mathfrak{J}}^L(o) &= \xi_{\mathfrak{H}}^L(o), \xi_{\mathfrak{J}}^U(o) = \xi_{\mathfrak{H}}^U(o), \\ \varsigma_{\mathfrak{J}}^L(o) &= \varsigma_{\mathfrak{H}}^L(o), \varsigma_{\mathfrak{J}}^U(o) = \varsigma_{\mathfrak{H}}^U(o), \\ \zeta_{\mathfrak{J}}^L(o) &= \zeta_{\mathfrak{H}}^L(o), \zeta_{\mathfrak{J}}^U(o) = \zeta_{\mathfrak{H}}^U(o).\end{aligned}$$

Hence, it can be deduced that $\mathfrak{J} = \mathfrak{H}$.

Therefore, we can prove that $\tilde{\mathbb{D}}_{IvPFS}^1(\mathfrak{J}, \mathfrak{H}) = 0$ if and only if $\mathfrak{J} = \mathfrak{H}$. \square

Proof: We know that

$$\tilde{\mathbb{D}}_{IvPFS}^1(\mathfrak{J}, \mathfrak{H}) = \frac{1}{n} \sum_{i=1}^n \sqrt{\frac{1}{4} \left(\begin{aligned} &\xi_{\mathfrak{J}}^L(o_i) \log \frac{2\xi_{\mathfrak{J}}^L(o_i)}{\xi_{\mathfrak{J}}^L(o_i) + \xi_{\mathfrak{H}}^L(o_i)} + \xi_{\mathfrak{J}}^U(o_i) \log \frac{2\xi_{\mathfrak{J}}^U(o_i)}{\xi_{\mathfrak{J}}^U(o_i) + \xi_{\mathfrak{H}}^U(o_i)} \\ &+ \xi_{\mathfrak{H}}^L(o_i) \log \frac{2\xi_{\mathfrak{H}}^L(o_i)}{\xi_{\mathfrak{J}}^L(o_i) + \xi_{\mathfrak{H}}^L(o_i)} + \xi_{\mathfrak{H}}^U(o_i) \log \frac{2\xi_{\mathfrak{H}}^U(o_i)}{\xi_{\mathfrak{J}}^U(o_i) + \xi_{\mathfrak{H}}^U(o_i)} \\ &\varsigma_{\mathfrak{J}}^L(o_i) \log \frac{2\varsigma_{\mathfrak{J}}^L(o_i)}{\varsigma_{\mathfrak{J}}^L(o_i) + \varsigma_{\mathfrak{H}}^L(o_i)} + \varsigma_{\mathfrak{J}}^U(o_i) \log \frac{2\varsigma_{\mathfrak{J}}^U(o_i)}{\varsigma_{\mathfrak{J}}^U(o_i) + \varsigma_{\mathfrak{H}}^U(o_i)} \\ &+ \varsigma_{\mathfrak{H}}^L(o_i) \log \frac{2\varsigma_{\mathfrak{H}}^L(o_i)}{\varsigma_{\mathfrak{J}}^L(o_i) + \varsigma_{\mathfrak{H}}^L(o_i)} + \varsigma_{\mathfrak{H}}^U(o_i) \log \frac{2\varsigma_{\mathfrak{H}}^U(o_i)}{\varsigma_{\mathfrak{J}}^U(o_i) + \varsigma_{\mathfrak{H}}^U(o_i)} \\ &\zeta_{\mathfrak{J}}^L(o_i) \log \frac{2\zeta_{\mathfrak{J}}^L(o_i)}{\zeta_{\mathfrak{J}}^L(o_i) + \zeta_{\mathfrak{H}}^L(o_i)} + \zeta_{\mathfrak{J}}^U(o_i) \log \frac{2\zeta_{\mathfrak{J}}^U(o_i)}{\zeta_{\mathfrak{J}}^U(o_i) + \zeta_{\mathfrak{H}}^U(o_i)} \\ &+ \zeta_{\mathfrak{H}}^L(o_i) \log \frac{2\zeta_{\mathfrak{H}}^L(o_i)}{\zeta_{\mathfrak{J}}^L(o_i) + \zeta_{\mathfrak{H}}^L(o_i)} + \zeta_{\mathfrak{H}}^U(o_i) \log \frac{2\zeta_{\mathfrak{H}}^U(o_i)}{\zeta_{\mathfrak{J}}^U(o_i) + \zeta_{\mathfrak{H}}^U(o_i)} \end{aligned} \right)}$$

$$\begin{aligned}
&= \frac{1}{n} \sum_{i=1}^n \sqrt{\frac{1}{4} \left(\begin{aligned} &\xi_{\mathfrak{J}}^L(\mathfrak{o}_i) \log \frac{2\xi_{\mathfrak{J}}^L(\mathfrak{o}_i)}{\xi_{\mathfrak{J}}^L(\mathfrak{o}_i) + \xi_{\mathfrak{H}}^L(\mathfrak{o}_i)} + \xi_{\mathfrak{H}}^U(\mathfrak{o}_i) \log \frac{2\xi_{\mathfrak{H}}^U(\mathfrak{o}_i)}{\xi_{\mathfrak{J}}^U(\mathfrak{o}_i) + \xi_{\mathfrak{H}}^U(\mathfrak{o}_i)} \\ &+ \xi_{\mathfrak{J}}^L(\mathfrak{o}_i) \log \frac{2\xi_{\mathfrak{J}}^L(\mathfrak{o}_i)}{\xi_{\mathfrak{J}}^L(\mathfrak{o}_i) + \xi_{\mathfrak{H}}^L(\mathfrak{o}_i)} + \xi_{\mathfrak{J}}^U(\mathfrak{o}_i) \log \frac{2\xi_{\mathfrak{J}}^U(\mathfrak{o}_i)}{\xi_{\mathfrak{J}}^U(\mathfrak{o}_i) + \xi_{\mathfrak{H}}^U(\mathfrak{o}_i)} \\ &\varsigma_{\mathfrak{J}}^L(\mathfrak{o}_i) \log \frac{2\varsigma_{\mathfrak{J}}^L(\mathfrak{o}_i)}{\varsigma_{\mathfrak{J}}^L(\mathfrak{o}_i) + \varsigma_{\mathfrak{H}}^L(\mathfrak{o}_i)} + \varsigma_{\mathfrak{H}}^U(\mathfrak{o}_i) \log \frac{2\varsigma_{\mathfrak{H}}^U(\mathfrak{o}_i)}{\varsigma_{\mathfrak{J}}^U(\mathfrak{o}_i) + \varsigma_{\mathfrak{H}}^U(\mathfrak{o}_i)} \\ &+ \varsigma_{\mathfrak{J}}^L(\mathfrak{o}_i) \log \frac{2\varsigma_{\mathfrak{J}}^L(\mathfrak{o}_i)}{\varsigma_{\mathfrak{J}}^L(\mathfrak{o}_i) + \varsigma_{\mathfrak{H}}^L(\mathfrak{o}_i)} + \varsigma_{\mathfrak{J}}^U(\mathfrak{o}_i) \log \frac{2\varsigma_{\mathfrak{J}}^U(\mathfrak{o}_i)}{\varsigma_{\mathfrak{J}}^U(\mathfrak{o}_i) + \varsigma_{\mathfrak{H}}^U(\mathfrak{o}_i)} \\ &\zeta_{\mathfrak{J}}^L(\mathfrak{o}_i) \log \frac{2\zeta_{\mathfrak{J}}^L(\mathfrak{o}_i)}{\zeta_{\mathfrak{J}}^L(\mathfrak{o}_i) + \zeta_{\mathfrak{H}}^L(\mathfrak{o}_i)} + \zeta_{\mathfrak{H}}^U(\mathfrak{o}_i) \log \frac{2\zeta_{\mathfrak{H}}^U(\mathfrak{o}_i)}{\zeta_{\mathfrak{J}}^U(\mathfrak{o}_i) + \zeta_{\mathfrak{H}}^U(\mathfrak{o}_i)} \\ &+ \zeta_{\mathfrak{J}}^L(\mathfrak{o}_i) \log \frac{2\zeta_{\mathfrak{J}}^L(\mathfrak{o}_i)}{\zeta_{\mathfrak{J}}^L(\mathfrak{o}_i) + \zeta_{\mathfrak{H}}^L(\mathfrak{o}_i)} + \zeta_{\mathfrak{J}}^U(\mathfrak{o}_i) \log \frac{2\zeta_{\mathfrak{J}}^U(\mathfrak{o}_i)}{\zeta_{\mathfrak{J}}^U(\mathfrak{o}_i) + \zeta_{\mathfrak{H}}^U(\mathfrak{o}_i)} \end{aligned} \right)} \\
&= \mathbb{D}_{IvPFS}^1(\mathfrak{H}, \mathfrak{J}).
\end{aligned}$$

As a result, we can obtain $\mathbb{D}_{IvPFS}(\mathfrak{J}, \mathfrak{H}) = \mathbb{D}_{IvPFS}(\mathfrak{H}, \mathfrak{J})$. \square

Proof: Four assumptions are proposed:

- Assumption 1: $\xi_{\mathfrak{J}}(\mathfrak{o}_i) \leq \xi_{\mathfrak{H}}(\mathfrak{o}_i) \leq \xi_{\mathcal{O}}(\mathfrak{o}_i)$.
- Assumption 2: $\xi_{\mathcal{O}}(\mathfrak{o}_i) \leq \xi_{\mathfrak{H}}(\mathfrak{o}_i) \leq \xi_{\mathfrak{J}}(\mathfrak{o}_i)$.
- Assumption 3: $\xi_{\mathfrak{H}}(\mathfrak{o}_i) \leq \min \{ \xi_{\mathfrak{J}}(\mathfrak{o}_i), \xi_{\mathcal{O}}(\mathfrak{o}_i) \}$.
- Assumption 4: $\xi_{\mathfrak{H}}(\mathfrak{o}_i) \geq \max \{ \xi_{\mathfrak{J}}(\mathfrak{o}_i), \xi_{\mathcal{O}}(\mathfrak{o}_i) \}$.

From Assumption 1, we can prove that

$$\begin{aligned}
&|\xi_{\mathfrak{J}}(\mathfrak{o}_i) - \xi_{\mathfrak{H}}(\mathfrak{o}_i)| + |\xi_{\mathfrak{H}}(\mathfrak{o}_i) - \xi_{\mathcal{O}}(\mathfrak{o}_i)| - |\xi_{\mathfrak{J}}(\mathfrak{o}_i) - \xi_{\mathcal{O}}(\mathfrak{o}_i)| \\
&= \xi_{\mathfrak{J}}(\mathfrak{o}_i) - \xi_{\mathfrak{H}}(\mathfrak{o}_i) + \xi_{\mathcal{O}}(\mathfrak{o}_i) - \xi_{\mathfrak{H}}(\mathfrak{o}_i) + \xi_{\mathfrak{J}}(\mathfrak{o}_i) - \xi_{\mathcal{O}}(\mathfrak{o}_i) \\
&= 0.
\end{aligned}$$

Given this Assumption 2, the proof is structured as follows:

$$\begin{aligned}
&|\xi_{\mathfrak{J}}(\mathfrak{o}_i) - \xi_{\mathfrak{H}}(\mathfrak{o}_i)| + |\xi_{\mathfrak{H}}(\mathfrak{o}_i) - \xi_{\mathcal{O}}(\mathfrak{o}_i)| - |\xi_{\mathfrak{J}}(\mathfrak{o}_i) - \xi_{\mathcal{O}}(\mathfrak{o}_i)| \\
&= \xi_{\mathfrak{J}}(\mathfrak{o}_i) - \xi_{\mathfrak{H}}(\mathfrak{o}_i) + \xi_{\mathfrak{H}}(\mathfrak{o}_i) - \xi_{\mathcal{O}}(\mathfrak{o}_i) - \xi_{\mathfrak{J}}(\mathfrak{o}_i) + \xi_{\mathcal{O}}(\mathfrak{o}_i) \\
&= 0.
\end{aligned}$$

The proof under Assumption 3 is as follows:

Obviously, it is known that $\xi_{\mathfrak{J}}(\mathfrak{o}_i) \geq \xi_{\mathfrak{H}}(\mathfrak{o}_i)$ and $\xi_{\mathcal{O}}(\mathfrak{o}_i) \geq \xi_{\mathfrak{H}}(\mathfrak{o}_i)$.

$$\begin{aligned}
&|\xi_{\mathfrak{J}}(\mathfrak{o}_i) - \xi_{\mathfrak{H}}(\mathfrak{o}_i)| + |\xi_{\mathfrak{H}}(\mathfrak{o}_i) - \xi_{\mathcal{O}}(\mathfrak{o}_i)| - |\xi_{\mathfrak{J}}(\mathfrak{o}_i) - \xi_{\mathcal{O}}(\mathfrak{o}_i)| \\
&= \begin{cases} \xi_{\mathfrak{J}}(\mathfrak{o}_i) - \xi_{\mathfrak{H}}(\mathfrak{o}_i) + \xi_{\mathcal{O}}(\mathfrak{o}_i) - \xi_{\mathfrak{H}}(\mathfrak{o}_i) - \xi_{\mathfrak{J}}(\mathfrak{o}_i) + \xi_{\mathcal{O}}(\mathfrak{o}_i) \\ \quad \text{if } \xi_{\mathcal{O}}(\mathfrak{o}_i) \leq \xi_{\mathfrak{J}}(\mathfrak{o}_i) \\ \xi_{\mathfrak{J}}(\mathfrak{o}_i) - \xi_{\mathfrak{H}}(\mathfrak{o}_i) + \xi_{\mathcal{O}}(\mathfrak{o}_i) - \xi_{\mathfrak{H}}(\mathfrak{o}_i) + \xi_{\mathfrak{J}}(\mathfrak{o}_i) - \xi_{\mathcal{O}}(\mathfrak{o}_i) \\ \quad \text{if } \xi_{\mathcal{O}}(\mathfrak{o}_i) > \xi_{\mathfrak{J}}(\mathfrak{o}_i) \end{cases} \\
&= 2(\min \{ \xi_{\mathfrak{J}}(\mathfrak{o}_i), \xi_{\mathcal{O}}(\mathfrak{o}_i) \} - \xi_{\mathfrak{H}}(\mathfrak{o}_i)) \geq 0.
\end{aligned}$$

The proof based on Assumption 4 is given below:

Likewise, it can be shown that $\xi_{\mathfrak{J}}(\mathfrak{o}_i) \leq \xi_{\mathfrak{H}}(\mathfrak{o}_i)$ and $\xi_{\mathcal{O}}(\mathfrak{o}_i) \leq \xi_{\mathfrak{H}}(\mathfrak{o}_i)$.

$$|\xi_{\mathfrak{J}}(\mathfrak{o}_i) - \xi_{\mathfrak{H}}(\mathfrak{o}_i)| + |\xi_{\mathfrak{H}}(\mathfrak{o}_i) - \xi_{\mathcal{O}}(\mathfrak{o}_i)| - |\xi_{\mathfrak{J}}(\mathfrak{o}_i) - \xi_{\mathcal{O}}(\mathfrak{o}_i)|$$

$$\begin{aligned}
&= \begin{cases} \xi_{\mathfrak{H}}(\mathfrak{o}_i) - \xi_{\mathfrak{J}}(\mathfrak{o}_i) + \xi_{\mathfrak{H}}(\mathfrak{o}_i) - \xi_{\mathcal{O}}(\mathfrak{o}_i) - \xi_{\mathfrak{J}}(\mathfrak{o}_i) + \xi_{\mathcal{O}}(\mathfrak{o}_i) \\ \text{if } \xi_{\mathcal{O}}(\mathfrak{o}_i) \leq \xi_{\mathfrak{J}}(\mathfrak{o}_i) \\ \xi_{\mathfrak{H}}(\mathfrak{o}_i) - \xi_{\mathfrak{J}}(\mathfrak{o}_i) + \xi_{\mathfrak{H}}(\mathfrak{o}_i) - \xi_{\mathcal{O}}(\mathfrak{o}_i) + \xi_{\mathfrak{J}}(\mathfrak{o}_i) - \xi_{\mathcal{O}}(\mathfrak{o}_i) \\ \text{if } \xi_{\mathcal{O}}(\mathfrak{o}_i) > \xi_{\mathfrak{J}}(\mathfrak{o}_i) \end{cases} \\
&= 2(\xi_{\mathfrak{H}}(\mathfrak{o}_i) - \max\{\xi_{\mathfrak{J}}(\mathfrak{o}_i), \xi_{\mathcal{O}}(\mathfrak{o}_i)\}) \geq 0.
\end{aligned}$$

In conclusion, under these four assumptions, we have proven that

$$|\xi_{\mathfrak{J}}(\mathfrak{o}_i) - \xi_{\mathfrak{H}}(\mathfrak{o}_i)| + |\xi_{\mathfrak{H}}(\mathfrak{o}_i) - \xi_{\mathcal{O}}(\mathfrak{o}_i)| \geq |\xi_{\mathfrak{J}}(\mathfrak{o}_i) - \xi_{\mathcal{O}}(\mathfrak{o}_i)|.$$

By the same reasoning, it follows that

$$\begin{aligned}
&|\varsigma_{\mathfrak{J}}(\mathfrak{o}_i) - \varsigma_{\mathfrak{H}}(\mathfrak{o}_i)| + |\varsigma_{\mathfrak{H}}(\mathfrak{o}_i) - \varsigma_{\mathcal{O}}(\mathfrak{o}_i)| \geq |\varsigma_{\mathfrak{J}}(\mathfrak{o}_i) - \varsigma_{\mathcal{O}}(\mathfrak{o}_i)|, \\
&|\zeta_{\mathfrak{J}}(\mathfrak{o}_i) - \zeta_{\mathfrak{H}}(\mathfrak{o}_i)| + |\zeta_{\mathfrak{H}}(\mathfrak{o}_i) - \zeta_{\mathcal{O}}(\mathfrak{o}_i)| \geq |\zeta_{\mathfrak{J}}(\mathfrak{o}_i) - \zeta_{\mathcal{O}}(\mathfrak{o}_i)|.
\end{aligned}$$

Hence, it can be seen that $\tilde{\mathbb{D}}_{IvPFS}^1(\mathfrak{J}, \mathfrak{H}) + \tilde{\mathbb{D}}_{IvPFS}^1(\mathfrak{H}, \mathcal{O}) \geq \tilde{\mathbb{D}}_{IvPFS}^1(\mathfrak{J}, \mathcal{O})$. \square

Proof: Suppose that \mathfrak{J} and \mathfrak{H} are two IvPFSs.

$$\begin{aligned}
\tilde{\mathbb{D}}_{IvPFS}^1(\mathfrak{J}, \mathfrak{H}) &= \frac{1}{n} \sum_{i=1}^n \sqrt{\frac{1}{4} \left(\begin{aligned} &\xi_{\mathfrak{J}}^L(\mathfrak{o}_i) \log \frac{2\xi_{\mathfrak{J}}^L(\mathfrak{o}_i)}{\xi_{\mathfrak{J}}^L(\mathfrak{o}_i) + \xi_{\mathfrak{H}}^L(\mathfrak{o}_i)} + \xi_{\mathfrak{J}}^U(\mathfrak{o}_i) \log \frac{2\xi_{\mathfrak{J}}^U(\mathfrak{o}_i)}{\xi_{\mathfrak{J}}^U(\mathfrak{o}_i) + \xi_{\mathfrak{H}}^U(\mathfrak{o}_i)} \\ &+ \xi_{\mathfrak{H}}^L(\mathfrak{o}_i) \log \frac{2\xi_{\mathfrak{H}}^L(\mathfrak{o}_i)}{\xi_{\mathfrak{J}}^L(\mathfrak{o}_i) + \xi_{\mathfrak{H}}^L(\mathfrak{o}_i)} + \xi_{\mathfrak{H}}^U(\mathfrak{o}_i) \log \frac{2\xi_{\mathfrak{H}}^U(\mathfrak{o}_i)}{\xi_{\mathfrak{J}}^U(\mathfrak{o}_i) + \xi_{\mathfrak{H}}^U(\mathfrak{o}_i)} \\ &\varsigma_{\mathfrak{J}}^L(\mathfrak{o}_i) \log \frac{2\varsigma_{\mathfrak{J}}^L(\mathfrak{o}_i)}{\varsigma_{\mathfrak{J}}^L(\mathfrak{o}_i) + \varsigma_{\mathfrak{H}}^L(\mathfrak{o}_i)} + \varsigma_{\mathfrak{J}}^U(\mathfrak{o}_i) \log \frac{2\varsigma_{\mathfrak{J}}^U(\mathfrak{o}_i)}{\varsigma_{\mathfrak{J}}^U(\mathfrak{o}_i) + \varsigma_{\mathfrak{H}}^U(\mathfrak{o}_i)} \\ &+ \varsigma_{\mathfrak{H}}^L(\mathfrak{o}_i) \log \frac{2\varsigma_{\mathfrak{H}}^L(\mathfrak{o}_i)}{\varsigma_{\mathfrak{J}}^L(\mathfrak{o}_i) + \varsigma_{\mathfrak{H}}^L(\mathfrak{o}_i)} + \varsigma_{\mathfrak{H}}^U(\mathfrak{o}_i) \log \frac{2\varsigma_{\mathfrak{H}}^U(\mathfrak{o}_i)}{\varsigma_{\mathfrak{J}}^U(\mathfrak{o}_i) + \varsigma_{\mathfrak{H}}^U(\mathfrak{o}_i)} \\ &\zeta_{\mathfrak{J}}^L(\mathfrak{o}_i) \log \frac{2\zeta_{\mathfrak{J}}^L(\mathfrak{o}_i)}{\zeta_{\mathfrak{J}}^L(\mathfrak{o}_i) + \zeta_{\mathfrak{H}}^L(\mathfrak{o}_i)} + \zeta_{\mathfrak{J}}^U(\mathfrak{o}_i) \log \frac{2\zeta_{\mathfrak{J}}^U(\mathfrak{o}_i)}{\zeta_{\mathfrak{J}}^U(\mathfrak{o}_i) + \zeta_{\mathfrak{H}}^U(\mathfrak{o}_i)} \\ &+ \zeta_{\mathfrak{H}}^L(\mathfrak{o}_i) \log \frac{2\zeta_{\mathfrak{H}}^L(\mathfrak{o}_i)}{\zeta_{\mathfrak{J}}^L(\mathfrak{o}_i) + \zeta_{\mathfrak{H}}^L(\mathfrak{o}_i)} + \zeta_{\mathfrak{H}}^U(\mathfrak{o}_i) \log \frac{2\zeta_{\mathfrak{H}}^U(\mathfrak{o}_i)}{\zeta_{\mathfrak{J}}^U(\mathfrak{o}_i) + \zeta_{\mathfrak{H}}^U(\mathfrak{o}_i)} \end{aligned} \right)}
\end{aligned}$$

$$\begin{aligned}
&= \frac{1}{n} \sum_{i=1}^n \sqrt{\frac{1}{4} \left(\begin{aligned}
&\left(\xi_{\mathfrak{J}}^L(\mathfrak{o}_i) + \xi_{\mathfrak{H}}^L(\mathfrak{o}_i) \right) \left(\frac{\xi_{\mathfrak{J}}^L(\mathfrak{o}_i)}{\xi_{\mathfrak{J}}^L(\mathfrak{o}_i) + \xi_{\mathfrak{H}}^L(\mathfrak{o}_i)} \log \frac{2\xi_{\mathfrak{J}}^L(\mathfrak{o}_i)}{\xi_{\mathfrak{J}}^L(\mathfrak{o}_i) + \xi_{\mathfrak{H}}^L(\mathfrak{o}_i)} \right. \\
&\quad \left. + \frac{\xi_{\mathfrak{H}}^L(\mathfrak{o}_i)}{\xi_{\mathfrak{J}}^L(\mathfrak{o}_i) + \xi_{\mathfrak{H}}^L(\mathfrak{o}_i)} \log \frac{2\xi_{\mathfrak{H}}^L(\mathfrak{o}_i)}{\xi_{\mathfrak{J}}^L(\mathfrak{o}_i) + \xi_{\mathfrak{H}}^L(\mathfrak{o}_i)} \right) \\
&+ \left(\xi_{\mathfrak{J}}^U(\mathfrak{o}_i) + \xi_{\mathfrak{H}}^U(\mathfrak{o}_i) \right) \left(\frac{\xi_{\mathfrak{J}}^U(\mathfrak{o}_i)}{\xi_{\mathfrak{J}}^U(\mathfrak{o}_i) + \xi_{\mathfrak{H}}^U(\mathfrak{o}_i)} \log \frac{2\xi_{\mathfrak{J}}^U(\mathfrak{o}_i)}{\xi_{\mathfrak{J}}^U(\mathfrak{o}_i) + \xi_{\mathfrak{H}}^U(\mathfrak{o}_i)} \right. \\
&\quad \left. + \frac{\xi_{\mathfrak{H}}^U(\mathfrak{o}_i)}{\xi_{\mathfrak{J}}^U(\mathfrak{o}_i) + \xi_{\mathfrak{H}}^U(\mathfrak{o}_i)} \log \frac{2\xi_{\mathfrak{H}}^U(\mathfrak{o}_i)}{\xi_{\mathfrak{J}}^U(\mathfrak{o}_i) + \xi_{\mathfrak{H}}^U(\mathfrak{o}_i)} \right) \\
&+ \left(\varsigma_{\mathfrak{J}}^L(\mathfrak{o}_i) + \varsigma_{\mathfrak{H}}^L(\mathfrak{o}_i) \right) \left(\frac{\varsigma_{\mathfrak{J}}^L(\mathfrak{o}_i)}{\varsigma_{\mathfrak{J}}^L(\mathfrak{o}_i) + \varsigma_{\mathfrak{H}}^L(\mathfrak{o}_i)} \log \frac{2\varsigma_{\mathfrak{J}}^L(\mathfrak{o}_i)}{\varsigma_{\mathfrak{J}}^L(\mathfrak{o}_i) + \varsigma_{\mathfrak{H}}^L(\mathfrak{o}_i)} \right. \\
&\quad \left. + \frac{\varsigma_{\mathfrak{H}}^L(\mathfrak{o}_i)}{\varsigma_{\mathfrak{J}}^L(\mathfrak{o}_i) + \varsigma_{\mathfrak{H}}^L(\mathfrak{o}_i)} \log \frac{2\varsigma_{\mathfrak{H}}^L(\mathfrak{o}_i)}{\varsigma_{\mathfrak{J}}^L(\mathfrak{o}_i) + \varsigma_{\mathfrak{H}}^L(\mathfrak{o}_i)} \right) \\
&+ \left(\varsigma_{\mathfrak{J}}^U(\mathfrak{o}_i) + \varsigma_{\mathfrak{H}}^U(\mathfrak{o}_i) \right) \left(\frac{\varsigma_{\mathfrak{J}}^U(\mathfrak{o}_i)}{\varsigma_{\mathfrak{J}}^U(\mathfrak{o}_i) + \varsigma_{\mathfrak{H}}^U(\mathfrak{o}_i)} \log \frac{2\varsigma_{\mathfrak{J}}^U(\mathfrak{o}_i)}{\varsigma_{\mathfrak{J}}^U(\mathfrak{o}_i) + \varsigma_{\mathfrak{H}}^U(\mathfrak{o}_i)} \right. \\
&\quad \left. + \frac{\varsigma_{\mathfrak{H}}^U(\mathfrak{o}_i)}{\varsigma_{\mathfrak{J}}^U(\mathfrak{o}_i) + \varsigma_{\mathfrak{H}}^U(\mathfrak{o}_i)} \log \frac{2\varsigma_{\mathfrak{H}}^U(\mathfrak{o}_i)}{\varsigma_{\mathfrak{J}}^U(\mathfrak{o}_i) + \varsigma_{\mathfrak{H}}^U(\mathfrak{o}_i)} \right) \\
&+ \left(\zeta_{\mathfrak{J}}^L(\mathfrak{o}_i) + \zeta_{\mathfrak{H}}^L(\mathfrak{o}_i) \right) \left(\frac{\zeta_{\mathfrak{J}}^L(\mathfrak{o}_i)}{\zeta_{\mathfrak{J}}^L(\mathfrak{o}_i) + \zeta_{\mathfrak{H}}^L(\mathfrak{o}_i)} \log \frac{2\zeta_{\mathfrak{J}}^L(\mathfrak{o}_i)}{\zeta_{\mathfrak{J}}^L(\mathfrak{o}_i) + \zeta_{\mathfrak{H}}^L(\mathfrak{o}_i)} \right. \\
&\quad \left. + \frac{\zeta_{\mathfrak{H}}^L(\mathfrak{o}_i)}{\zeta_{\mathfrak{J}}^L(\mathfrak{o}_i) + \zeta_{\mathfrak{H}}^L(\mathfrak{o}_i)} \log \frac{2\zeta_{\mathfrak{H}}^L(\mathfrak{o}_i)}{\zeta_{\mathfrak{J}}^L(\mathfrak{o}_i) + \zeta_{\mathfrak{H}}^L(\mathfrak{o}_i)} \right) \\
&+ \left(\zeta_{\mathfrak{J}}^U(\mathfrak{o}_i) + \zeta_{\mathfrak{H}}^U(\mathfrak{o}_i) \right) \left(\frac{\zeta_{\mathfrak{J}}^U(\mathfrak{o}_i)}{\zeta_{\mathfrak{J}}^U(\mathfrak{o}_i) + \zeta_{\mathfrak{H}}^U(\mathfrak{o}_i)} \log \frac{2\zeta_{\mathfrak{J}}^U(\mathfrak{o}_i)}{\zeta_{\mathfrak{J}}^U(\mathfrak{o}_i) + \zeta_{\mathfrak{H}}^U(\mathfrak{o}_i)} \right. \\
&\quad \left. + \frac{\zeta_{\mathfrak{H}}^U(\mathfrak{o}_i)}{\zeta_{\mathfrak{J}}^U(\mathfrak{o}_i) + \zeta_{\mathfrak{H}}^U(\mathfrak{o}_i)} \log \frac{2\zeta_{\mathfrak{H}}^U(\mathfrak{o}_i)}{\zeta_{\mathfrak{J}}^U(\mathfrak{o}_i) + \zeta_{\mathfrak{H}}^U(\mathfrak{o}_i)} \right)
\end{aligned} \right)
\end{aligned}$$

$$= \frac{1}{n} \sum_{i=1}^n \sqrt{\frac{1}{4} (\mathfrak{J} + \mathfrak{H}) \left(1 - H \left(\frac{\mathfrak{J}}{\mathfrak{J} + \mathfrak{H}}, \frac{\mathfrak{H}}{\mathfrak{J} + \mathfrak{H}} \right) \right)}.$$

For each $\xi \in [0, 1]$,

$$1 - H(\xi, 1 - \xi) \leq |\xi - (1 - \xi)|.$$

When $n = 1$, it is defined as $\mathbb{D}_{IvPFS}^1(\mathfrak{J}, \mathfrak{H})$. Then, we can get:

$$\mathbb{D}_{IvPFS}^1(\mathfrak{J}, \mathfrak{H}) \leq \left[\frac{1}{4} (\mathfrak{J} + \mathfrak{H}) \left| \frac{\mathfrak{J}}{\mathfrak{J} + \mathfrak{H}}, \frac{\mathfrak{H}}{\mathfrak{J} + \mathfrak{H}} \right| \right]^{\frac{1}{2}} = \left[\frac{1}{4} V(\mathfrak{J}, \mathfrak{H}) \right]^{\frac{1}{2}}$$

where $V(\mathfrak{J}, \mathfrak{H})$ is the variational distance of $\mathfrak{J}, \mathfrak{H}$. We can prove that $0 \leq V(\mathfrak{J}, \mathfrak{H}) \leq 4$.

Therefore, it is proven that $0 \leq \mathbb{D}_{IvPFS}(\mathfrak{J}, \mathfrak{H}) \leq 1$. \square

4 Numerical Comparisons

This section shows four numerical examples to demonstrate the introduced divergence measures.

Example 1. Consider three IvPFSs \mathfrak{J} , \mathfrak{H} , and \mathcal{O} as follows:

$$\mathfrak{J} = \{ \langle [0.12, 0.37], [0.29, 0.31], [0.26, 0.27] \rangle \},$$

$$\mathfrak{H} = \{ \langle [0.12, 0.37], [0.29, 0.31], [0.26, 0.27] \rangle \},$$

$$\mathcal{O} = \{ \langle [0.50, 0.55], [0.17, 0.21], [0.15, 0.21] \rangle \}.$$

We can compute the divergence measures between these IvPFSs as follows:

$$\mathbb{D}_{IvPFS}^1(\mathfrak{J}, \mathfrak{H}) = 0.0000, \mathbb{D}_{IvPFS}^1(\mathfrak{H}, \mathfrak{J}) = 0.0000,$$

$$\begin{aligned}\tilde{\mathbb{D}}_{IvPFS}^2(\mathfrak{J}, \mathfrak{H}) &= 0.0000, \tilde{\mathbb{D}}_{IvPFS}^2(\mathfrak{H}, \mathfrak{J}) = 0.0000, \\ \tilde{\mathbb{D}}_{IvPFS}^1(\mathfrak{J}, \mathcal{O}) &= 0.2163, \tilde{\mathbb{D}}_{IvPFS}^1(\mathcal{O}, \mathfrak{J}) = 0.2163, \\ \tilde{\mathbb{D}}_{IvPFS}^2(\mathfrak{J}, \mathcal{O}) &= 0.2302, \tilde{\mathbb{D}}_{IvPFS}^2(\mathcal{O}, \mathfrak{J}) = 0.2302.\end{aligned}$$

These results demonstrate that both divergence measures, $\tilde{\mathbb{D}}_{IvPFS}^1$ and $\tilde{\mathbb{D}}_{IvPFS}^2$, satisfy the Property 1 and Property 1 as expected.

Example 2. Consider three interval-valued Picture fuzzy sets (IvPFSs) \mathfrak{J} , \mathfrak{H} , and \mathcal{O} defined as follows:

$$\begin{aligned}\mathfrak{J} &= \{\langle [0.09, 0.28], [0.47, 0.48], [0.16, 0.19] \rangle\}, \\ \mathfrak{H} &= \{\langle [0.11, 0.17], [0.24, 0.33], [0.29, 0.30] \rangle\}, \\ \mathcal{O} &= \{\langle [0.10, 0.22], [0.04, 0.28], [0.48, 0.48] \rangle\}.\end{aligned}$$

The computed divergence measures between these IvPFSs are as follows:

$$\begin{aligned}\tilde{\mathbb{D}}_{IvPFS}^1(\mathfrak{J}, \mathfrak{H}) &= 0.1565, \tilde{\mathbb{D}}_{IvPFS}^1(\mathfrak{H}, \mathcal{O}) = 0.1799, \\ \tilde{\mathbb{D}}_{IvPFS}^1(\mathfrak{J}, \mathcal{O}) &= 0.3132, \tilde{\mathbb{D}}_{IvPFS}^2(\mathfrak{J}, \mathfrak{H}) = 0.1944, \\ \tilde{\mathbb{D}}_{IvPFS}^2(\mathfrak{H}, \mathcal{O}) &= 0.3280, \tilde{\mathbb{D}}_{IvPFS}^2(\mathfrak{J}, \mathcal{O}) = 0.2319.\end{aligned}$$

These results satisfy the triangular inequality property:

$$\tilde{\mathbb{D}}_{IvPFS}(\mathfrak{J}, \mathfrak{H}) + \tilde{\mathbb{D}}_{IvPFS}(\mathfrak{H}, \mathcal{O}) \geq \tilde{\mathbb{D}}_{IvPFS}(\mathfrak{J}, \mathcal{O}),$$

demonstrating that both divergence measures, $\tilde{\mathbb{D}}_{IvPFS}^1$ and $\tilde{\mathbb{D}}_{IvPFS}^2$, satisfy Property 3.

Example 3. For each Case_i (where $i = 1, 2, 3, 4$), the IvPFSs \mathfrak{J}_i and \mathfrak{H}_i are provided in Table 2. The corresponding results across these four cases are summarized in Table 3.

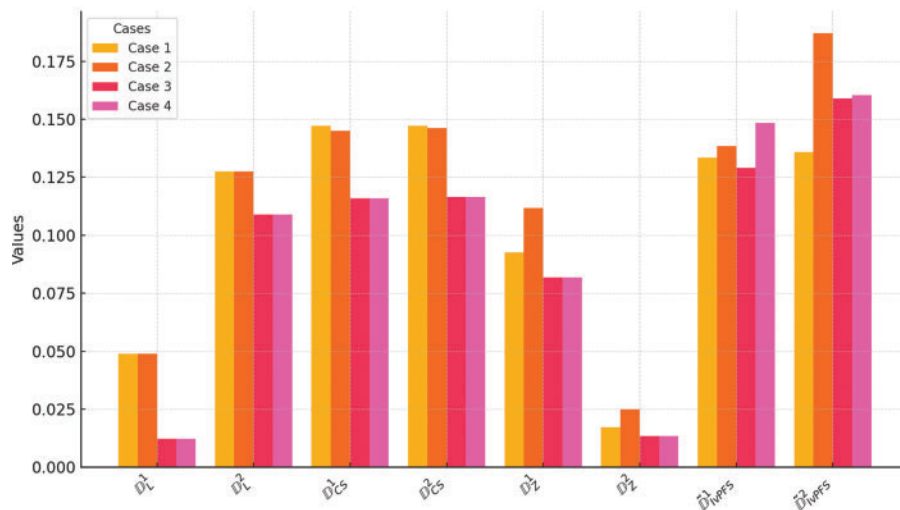
Table 2: The IvPFSs \mathfrak{J}_i and \mathfrak{H}_i are examined across different cases in example 3

IvPFSs	Case ₁	Case ₂
\mathfrak{J}_i	$\langle [0.40, 0.45], [0.10, 0.15], [0.30, 0.35] \rangle$	$\langle [0.25, 0.30], [0.05, 0.20], [0.45, 0.45] \rangle$
\mathfrak{H}_i	$\langle [0.20, 0.30], [0.15, 0.20], [0.40, 0.45] \rangle$	$\langle [0.15, 0.50], [0.10, 0.20], [0.30, 0.30] \rangle$
IvPFSs	Case ₃	Case ₄
\mathfrak{J}_i	$\langle [0.20, 0.30], [0.35, 0.35], [0.10, 0.20] \rangle$	$\langle [0.15, 0.25], [0.10, 0.15], [0.15, 0.30] \rangle$
\mathfrak{H}_i	$\langle [0.10, 0.20], [0.45, 0.45], [0.20, 0.30] \rangle$	$\langle [0.05, 0.15], [0.20, 0.25], [0.25, 0.40] \rangle$

The findings shown in Table 3 and illustrated in Fig. 2 indicate that the two proposed divergence measures for IvPFSs are particularly effective at distinguishing between different scenarios. However, in scenarios with highly similar instances, such as between Case₁ and Case₂, both \mathbb{D}_L^1 and \mathbb{D}_L^2 have identical results, indicating their limitations in distinguishing these cases effectively. A similar pattern with Case₃ and Case₄, where all six measures, \mathbb{D}_L^1 , \mathbb{D}_L^2 , \mathbb{D}_{CS}^1 , \mathbb{D}_{CS}^2 , \mathbb{D}_Z^1 , and \mathbb{D}_Z^2 , produce identical results. Despite these challenges, the proposed divergence measures prove more effective in capturing differences across cases.

Table 3: The evaluation of various measures for IvPFSs

	<i>Case₁</i>	<i>Case₂</i>	<i>Case₃</i>	<i>Case₄</i>
\mathbb{D}_L^1	0.0489	0.0489	0.0123	0.0123
\mathbb{D}_L^2	0.1275	0.1275	0.1090	0.1090
\mathbb{D}_{CS}^1	0.1472	0.1451	0.1159	0.1159
\mathbb{D}_{CS}^2	0.1473	0.1463	0.1166	0.1166
\mathbb{D}_Z^1	0.0926	0.1118	0.0818	0.0818
\mathbb{D}_Z^2	0.0172	0.0250	0.0134	0.0134
$\tilde{\mathbb{D}}_{IvPFS}^1$	0.1334	0.1384	0.1291	0.1485
$\tilde{\mathbb{D}}_{IvPFS}^2$	0.1359	0.1872	0.1590	0.1604

**Figure 2:** The comparison between existing measures and proposed measures in example 3

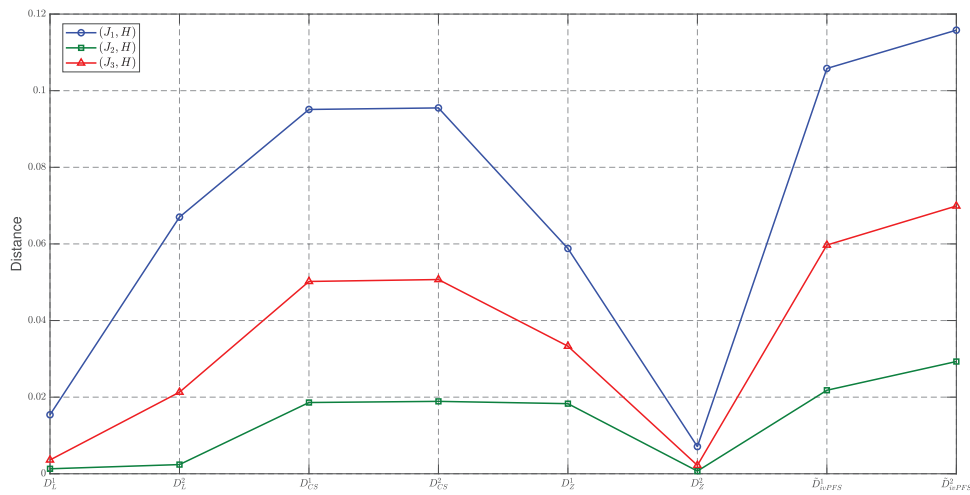
Example 4. Consider three known patterns \mathfrak{J}_1 , \mathfrak{J}_2 , and \mathfrak{J}_3 , along with the unknown pattern \mathfrak{J}_4 , each characterized by properties described by IvPFSs within the feature space X . The data and results for these patterns are presented in Table 4 and Fig. 3.

$$\mathfrak{J}_1 = \left\{ \begin{array}{l} \left\langle \begin{array}{l} [0.20, 0.30], \\ [0.26, 0.30], \\ [0.15, 0.22] \end{array}, \begin{array}{l} [0.15, 0.24], \\ [0.18, 0.25], \\ [0.21, 0.30] \end{array} \right\rangle, \\ \left\langle \begin{array}{l} [0.18, 0.25], \\ [0.13, 0.25], \\ [0.20, 0.26] \end{array}, \begin{array}{l} [0.15, 0.24], \\ [0.15, 0.19], \\ [0.25, 0.30] \end{array} \right\rangle, \\ \left\langle \begin{array}{l} [0.20, 0.30], \\ [0.25, 0.28], \\ [0.10, 0.20] \end{array} \right\rangle \end{array} \right\}, \mathfrak{J}_2 = \left\{ \begin{array}{l} \left\langle \begin{array}{l} [0.26, 0.38], \\ [0.21, 0.25], \\ [0.12, 0.15] \end{array}, \begin{array}{l} [0.18, 0.29], \\ [0.24, 0.35], \\ [0.16, 0.23] \end{array} \right\rangle, \\ \left\langle \begin{array}{l} [0.24, 0.30], \\ [0.20, 0.29], \\ [0.12, 0.19] \end{array}, \begin{array}{l} [0.25, 0.30], \\ [0.18, 0.25], \\ [0.14, 0.20] \end{array} \right\rangle, \\ \left\langle \begin{array}{l} [0.34, 0.40], \\ [0.15, 0.20], \\ [0.18, 0.29] \end{array} \right\rangle \end{array} \right\},$$

$$\mathfrak{J}_3 = \left\{ \begin{array}{l} \left\langle \begin{bmatrix} 0.25, 0.35 \\ 0.15, 0.20 \\ 0.13, 0.19 \end{bmatrix}, \begin{bmatrix} 0.23, 0.35 \\ 0.20, 0.30 \\ 0.10, 0.25 \end{bmatrix} \right\rangle, \\ \left\langle \begin{bmatrix} 0.30, 0.35 \\ 0.15, 0.27 \\ 0.07, 0.17 \end{bmatrix}, \begin{bmatrix} 0.20, 0.25 \\ 0.24, 0.30 \\ 0.10, 0.16 \end{bmatrix} \right\rangle, \\ \left\langle \begin{bmatrix} 0.30, 0.38 \\ 0.20, 0.25 \\ 0.15, 0.26 \end{bmatrix} \right\rangle \end{array} \right\}, \mathfrak{H} = \left\{ \begin{array}{l} \left\langle \begin{bmatrix} 0.30, 0.40 \\ 0.20, 0.24 \\ 0.10, 0.15 \end{bmatrix}, \begin{bmatrix} 0.20, 0.30 \\ 0.25, 0.34 \\ 0.15, 0.21 \end{bmatrix} \right\rangle, \\ \left\langle \begin{bmatrix} 0.25, 0.32 \\ 0.21, 0.30 \\ 0.10, 0.20 \end{bmatrix}, \begin{bmatrix} 0.26, 0.31 \\ 0.20, 0.25 \\ 0.15, 0.21 \end{bmatrix} \right\rangle, \\ \left\langle \begin{bmatrix} 0.35, 0.42 \\ 0.16, 0.21 \\ 0.20, 0.30 \end{bmatrix} \right\rangle \end{array} \right\}.$$

Table 4: Results for pattern recognition under example 4

	$(\mathfrak{J}_1, \mathfrak{H})$	$(\mathfrak{J}_2, \mathfrak{H})$	$(\mathfrak{J}_3, \mathfrak{H})$	Result
\mathbb{D}_L^1	0.0154	0.0013	0.0036	\mathfrak{J}_2
\mathbb{D}_L^2	0.0670	0.0024	0.0213	\mathfrak{J}_2
\mathbb{D}_{CS}^1	0.0951	0.0186	0.0502	\mathfrak{J}_2
\mathbb{D}_{CS}^2	0.0955	0.0189	0.0507	\mathfrak{J}_2
\mathbb{D}_Z^1	0.0588	0.0183	0.0333	\mathfrak{J}_2
\mathbb{D}_Z^2	0.0071	0.0007	0.0022	\mathfrak{J}_2
$\tilde{\mathbb{D}}_{IvPFS}^1$	0.1058	0.0218	0.0597	\mathfrak{J}_2
$\tilde{\mathbb{D}}_{IvPFS}^2$	0.1158	0.0293	0.0699	\mathfrak{J}_2

**Figure 3:** The comparison between existing measures and proposed measures in example 4

Based on the results presented in Table 4, the following conclusion can be drawn: across all measures (\mathbb{D}_L^1 , \mathbb{D}_L^2 , \mathbb{D}_{CS}^1 , \mathbb{D}_{CS}^2 , \mathbb{D}_Z^1 , \mathbb{D}_Z^2 , $\tilde{\mathbb{D}}_{IvPFS}^1$ and $\tilde{\mathbb{D}}_{IvPFS}^2$), the unknown pattern \mathfrak{H} consistently shows the smallest distance to the known pattern \mathfrak{J}_2 , which indicates a high degree of similarity between them. This finding suggests that \mathfrak{J}_2 is the best match for \mathfrak{H} across all evaluated metrics, further validating the accuracy of \mathfrak{H} 's classification and the effectiveness of the model.

The divergence scores reflect the degree of dissimilarity between \mathfrak{H} and each reference pattern. A lower divergence value corresponds to a higher similarity and thus a stronger classification association. For instance, if $\tilde{\mathbb{D}}_{IvPFS}^1(\mathfrak{H}, \mathfrak{J}_i) < \tilde{\mathbb{D}}_{IvPFS}^1(\mathfrak{H}, \mathfrak{J}_k)$, this implies that pattern \mathfrak{H} shares more uncertainty characteristics with \mathfrak{J}_i than with \mathfrak{J}_k . This mapping logic enables the direct use of divergence measures as pattern similarity indicators in classification tasks. The classification decision for \mathfrak{H} is then made by assigning it to the pattern class with the lowest divergence, similar to nearest neighbor principles in metric spaces.

It is important to note their practical application. For instance, the IvPFSs in Example 3 and Example 4 can be viewed as abstract representations of expert evaluations in real-world scenarios, such as engineering risk levels, patient symptoms, or environmental assessments. Each component of the IvPFS corresponds to the interval-valued judgment on positive, negative, or neutral aspects of an alternative. Consequently, smaller divergence values indicate higher consistency in expert opinions or higher similarity in attributes.

5 Application

In this section, we will introduce an improved TOPSIS for a risk assessment in a construction project.

5.1 The Improved TOPSIS Approach

TOPSIS is a method used in MCDM to determine the optimal solution from multiple options. Its basic principle is to evaluate each option by comparing it with a positive ideal solution (PIS) and a negative ideal solution (NIS). Our improved TOPSIS method for IvPFSs is as follows:

- Step 1:** Define the performance of each alternative $P = \{P_1, P_2, \dots, P_m\}$ across multiple evaluation criteria $C = \{C_1, C_2, \dots, C_n\}$, forming a matrix $\mathcal{V} = (\hat{\mathbf{o}}_{ij})_{m \times n}$ containing these evaluation values which are represented as spherical fuzzy numbers $\hat{\mathbf{o}}_{ij} = \langle \xi_{ij}, \varsigma_{ij}, \zeta_{ij} \rangle$, where $\xi_{ij} = [\xi_{ij}^L, \xi_{ij}^U]$, $\varsigma_{ij} = [\varsigma_{ij}^L, \varsigma_{ij}^U]$ and $\zeta_{ij} = [\zeta_{ij}^L, \zeta_{ij}^U]$. It is defined as:

$$\mathcal{V} = (\hat{\mathbf{o}}_{ij})_{m \times n} = \begin{pmatrix} & C_1 & C_2 & \dots & C_n \\ P_1 & \langle [\xi_{11}^L, \xi_{11}^U], [\varsigma_{11}^L, \varsigma_{11}^U], [\zeta_{11}^L, \zeta_{11}^U] \rangle & \langle [\xi_{12}^L, \xi_{12}^U], [\varsigma_{12}^L, \varsigma_{12}^U], [\zeta_{12}^L, \zeta_{12}^U] \rangle & \dots & \langle [\xi_{1n}^L, \xi_{1n}^U], [\varsigma_{1n}^L, \varsigma_{1n}^U], [\zeta_{1n}^L, \zeta_{1n}^U] \rangle \\ P_2 & \langle [\xi_{21}^L, \xi_{21}^U], [\varsigma_{21}^L, \varsigma_{21}^U], [\zeta_{21}^L, \zeta_{21}^U] \rangle & \langle [\xi_{22}^L, \xi_{22}^U], [\varsigma_{22}^L, \varsigma_{22}^U], [\zeta_{22}^L, \zeta_{22}^U] \rangle & \dots & \langle [\xi_{2n}^L, \xi_{2n}^U], [\varsigma_{2n}^L, \varsigma_{2n}^U], [\zeta_{2n}^L, \zeta_{2n}^U] \rangle \\ \vdots & \vdots & \vdots & \ddots & \vdots \\ P_m & \langle [\xi_{m1}^L, \xi_{m1}^U], [\varsigma_{m1}^L, \varsigma_{m1}^U], [\zeta_{m1}^L, \zeta_{m1}^U] \rangle & \langle [\xi_{m2}^L, \xi_{m2}^U], [\varsigma_{m2}^L, \varsigma_{m2}^U], [\zeta_{m2}^L, \zeta_{m2}^U] \rangle & \dots & \langle [\xi_{mn}^L, \xi_{mn}^U], [\varsigma_{mn}^L, \varsigma_{mn}^U], [\zeta_{mn}^L, \zeta_{mn}^U] \rangle \end{pmatrix}.$$

- Step 2:** Based on the nature of each criterion, determine the PIS and NIS by selecting the maximum and minimum spherical fuzzy values for each criterion:

$$PIS = \hat{\mathbf{o}}^+ = (\hat{\mathbf{o}}_1^+, \hat{\mathbf{o}}_2^+, \hat{\mathbf{o}}_3^+, \hat{\mathbf{o}}_4^+, \hat{\mathbf{o}}_5^+),$$

$$NIS = \hat{\mathbf{o}}^- = (\hat{\mathbf{o}}_1^-, \hat{\mathbf{o}}_2^-, \hat{\mathbf{o}}_3^-, \hat{\mathbf{o}}_4^-, \hat{\mathbf{o}}_5^-).$$

Generally, \hat{o}_j^+ and \hat{o}_j^- are defined as follows:

$$\hat{o}_j^+ = \begin{cases} (\max_{1 \leq i \leq m} \{\xi_{ij}\}, \min_{1 \leq i \leq m} \{\varsigma_{ij}\}, \min_{1 \leq i \leq m} \{\zeta_{ij}\}) = (\xi_j^+, \varsigma_j^+, \zeta_j^+) & \text{if } \mathcal{O}_j \in \mathcal{O}^+ \\ (\min_{1 \leq i \leq m} \{\xi_{ij}\}, \max_{1 \leq i \leq m} \{\varsigma_{ij}\}, \max_{1 \leq i \leq m} \{\zeta_{ij}\}) = (\xi_j^-, \varsigma_j^-, \zeta_j^-) & \text{if } \mathcal{O}_j \in \mathcal{O}^- \end{cases}, \quad (11)$$

$$\hat{o}_j^- = \begin{cases} (\min_{1 \leq i \leq m} \{\xi_{ij}\}, \max_{1 \leq i \leq m} \{\varsigma_{ij}\}, \max_{1 \leq i \leq m} \{\zeta_{ij}\}) = (\xi_j^-, \varsigma_j^-, \zeta_j^-) & \text{if } \mathcal{O}_j \in \mathcal{O}^+ \\ (\max_{1 \leq i \leq m} \{\xi_{ij}\}, \min_{1 \leq i \leq m} \{\varsigma_{ij}\}, \min_{1 \leq i \leq m} \{\zeta_{ij}\}) = (\xi_j^+, \varsigma_j^+, \zeta_j^+) & \text{if } \mathcal{O}_j \in \mathcal{O}^- \end{cases}. \quad (12)$$

- **Step 3:** Calculate the separation of each alternative from the PIS and NIS, then generate the separation measures \mathcal{V}^+ and \mathcal{V}^- :

$$\mathcal{V}^+ = (D(\hat{o}_{ij}, \hat{o}_j^+))_{m \times n} = \begin{pmatrix} \mathcal{O}_1 & \mathcal{O}_2 & \cdots & \mathcal{O}_n \\ P_1 & D(\hat{o}_{11}, \hat{o}_1^+) & D(\hat{o}_{12}, \hat{o}_2^+) & \cdots & D(\hat{o}_{1n}, \hat{o}_n^+) \\ P_2 & D(\hat{o}_{21}, \hat{o}_1^+) & D(\hat{o}_{22}, \hat{o}_2^+) & \cdots & D(\hat{o}_{2n}, \hat{o}_n^+) \\ \vdots & \vdots & \vdots & \ddots & \vdots \\ P_m & D(\hat{o}_{m1}, \hat{o}_1^+) & D(\hat{o}_{m2}, \hat{o}_2^+) & \cdots & D(\hat{o}_{mn}, \hat{o}_n^+) \end{pmatrix}, \quad (13)$$

$$\mathcal{V}^- = (D(\hat{o}_{ij}, \hat{o}_j^-))_{m \times n} = \begin{pmatrix} \mathcal{O}_1 & \mathcal{O}_2 & \cdots & \mathcal{O}_n \\ P_1 & D(\hat{o}_{11}, \hat{o}_1^-) & D(\hat{o}_{12}, \hat{o}_2^-) & \cdots & D(\hat{o}_{1n}, \hat{o}_n^-) \\ P_2 & D(\hat{o}_{21}, \hat{o}_1^-) & D(\hat{o}_{22}, \hat{o}_2^-) & \cdots & D(\hat{o}_{2n}, \hat{o}_n^-) \\ \vdots & \vdots & \vdots & \ddots & \vdots \\ P_m & D(\hat{o}_{m1}, \hat{o}_1^-) & D(\hat{o}_{m2}, \hat{o}_2^-) & \cdots & D(\hat{o}_{mn}, \hat{o}_n^-) \end{pmatrix}. \quad (14)$$

- **Step 4:** For each alternative P_i and each criterion \mathcal{O}_i , compute a net distance \mathcal{S}_{ij}^* that reflects the difference between its distance to the PIS and its distance to the NIS. Combine all net distances into a matrix \mathcal{V}^* , called a spherical fuzzy distance matrix:

$$\begin{aligned} \mathcal{V}^* &= \mathcal{V}^+ - \mathcal{V}^- = (\mathcal{S}_{ij}^*)_{m \times n} \\ &= \begin{pmatrix} \mathcal{O}_1 & \mathcal{O}_2 & \cdots & \mathcal{O}_n \\ P_1 & \mathcal{S}_{11}^* & \mathcal{S}_{12}^* & \cdots & \mathcal{S}_{1n}^* \\ P_2 & \mathcal{S}_{21}^* & \mathcal{S}_{22}^* & \cdots & \mathcal{S}_{2n}^* \\ \vdots & \vdots & \vdots & \ddots & \vdots \\ P_m & \mathcal{S}_{m1}^* & \mathcal{S}_{m2}^* & \cdots & \mathcal{S}_{mn}^* \end{pmatrix} \\ &= \begin{pmatrix} \mathcal{O}_1 & \mathcal{O}_2 & \cdots & \mathcal{O}_n \\ P_1 & D(\hat{o}_{11}, \hat{o}_1^-) - D(\hat{o}_{11}, \hat{o}_1^+) & D(\hat{o}_{12}, \hat{o}_2^-) - D(\hat{o}_{12}, \hat{o}_2^+) & \cdots & D(\hat{o}_{1n}, \hat{o}_n^-) - D(\hat{o}_{1n}, \hat{o}_n^+) \\ P_2 & D(\hat{o}_{21}, \hat{o}_1^-) - D(\hat{o}_{21}, \hat{o}_1^+) & D(\hat{o}_{22}, \hat{o}_2^-) - D(\hat{o}_{22}, \hat{o}_2^+) & \cdots & D(\hat{o}_{2n}, \hat{o}_n^-) - D(\hat{o}_{2n}, \hat{o}_n^+) \\ \vdots & \vdots & \vdots & \ddots & \vdots \\ P_m & D(\hat{o}_{m1}, \hat{o}_1^-) - D(\hat{o}_{m1}, \hat{o}_1^+) & D(\hat{o}_{m2}, \hat{o}_2^-) - D(\hat{o}_{m2}, \hat{o}_2^+) & \cdots & D(\hat{o}_{mn}, \hat{o}_n^-) - D(\hat{o}_{mn}, \hat{o}_n^+) \end{pmatrix} \end{aligned} \quad (15)$$

- **Step 5:** Determine the weight of each criterion $w^* = (w_1, w_2, \dots, w_n)^T$ and calculate a weighted comprehensive score for each alternative \tilde{V}_i , reflecting its overall ranking:

$$\tilde{V}_i = \sum_{j=1}^n w_j^* \mathcal{S}_{ij}^*, i = 1, 2, \dots, m. \quad (16)$$

- **Step 6:** Rank the alternatives based on their relative closeness and select the one with the highest closeness as the optimal alternative.

5.2 Risk Assessment in Construction Project

5.2.1 Background

A construction company managing multiple projects wants to assess risks to ensure safety, profitability, and smooth operations. Because each project presents unique challenges, it is critical to systematically identify, evaluate, and prioritize risks. Proper risk assessment helps the company allocate resources efficiently and take preventive measures to mitigate potential threats.

The process accounts for uncertainty and incorporates objective and subjective judgments from stakeholders, including project managers, safety inspectors, financial analysts, and environmental experts.

The company evaluates four major ongoing projects:

- \mathcal{P}_1 : Residential construction.
- \mathcal{P}_2 : Commercial office construction.
- \mathcal{P}_3 : Infrastructure construction.
- \mathcal{P}_4 : Industrial warehouse construction.

The risk evaluation considers the following essential criteria:

- \mathcal{O}_1 : Safety Standards: weather conditions and accident risks.
- \mathcal{O}_2 : Financial Stability—maintaining budget discipline and avoiding cost overruns.
- \mathcal{O}_3 : Legal Compliance—adhering to regulations and minimizing legal disputes.
- \mathcal{O}_4 : Environmental Concerns: impact on the surrounding environment.
- \mathcal{O}_5 : Technical Challenges: complexity of engineering and technical solutions.

5.2.2 Modeling Assumptions and Data Preparation

In construction risk assessment, uncertainty frequently arises from fluctuating environmental, financial, and operational factors. To effectively capture this uncertainty, expert judgments on key risk indicators—such as cost overrun, schedule delay, and safety violations—are collected using linguistic terms.

Each alternative (i.e., construction project plan) is evaluated across five criteria within this IvPFS framework. To ensure logical consistency and model validity, a fuzzy consistency check is performed, and all fuzzy evaluations are normalized to satisfy the IvPFS constraint as mentioned in [Section 2](#).

The improved TOPSIS method proposed in this study incorporates the new divergence measures to provide a robust means of ranking alternatives by their proximity to the optimal risk profile under uncertain conditions. By integrating expert knowledge with fuzzy modeling of uncertainty, the proposed approach supports comprehensive, reliable decision-making and helps stakeholders prioritize risk mitigation strategies effectively.

5.2.3 Detailed Calculation Example

Let us consider our proposed divergence measure \mathbb{D}_{IVPFS}^1 .

- **Step 1:** To construct the decision matrix $\mathcal{V} = (\hat{\mathbf{d}}_{ij})_{4 \times 5}$, we use the interval-valued picture fuzzy numbers $\hat{\mathbf{d}}_{ij} = \langle \xi_{ij}, \varsigma_{ij}, \zeta_{ij} \rangle$, where $\xi_{ij} = [\xi_{ij}^L, \xi_{ij}^U]$, $\varsigma_{ij} = [\varsigma_{ij}^L, \varsigma_{ij}^U]$ and $\zeta_{ij} = [\zeta_{ij}^L, \zeta_{ij}^U]$ ($i = 1, 2, 3, 4, j = 1, 2, 3, 4, 5$).

$$\mathcal{V} = \begin{pmatrix} & \mathcal{O}_1 & \mathcal{O}_2 & \mathcal{O}_3 & \mathcal{P}_4 & \mathcal{O}_5 \\ \mathcal{P}_1 & \langle [0.23, 0.29], [0.20, 0.24], [0.12, 0.17] \rangle & \langle [0.21, 0.27], [0.22, 0.26], [0.10, 0.17] \rangle & \langle [0.18, 0.29], [0.17, 0.26], [0.13, 0.18] \rangle & \langle [0.20, 0.27], [0.25, 0.27], [0.25, 0.32] \rangle & \langle [0.20, 0.26], [0.23, 0.31], [0.27, 0.30] \rangle \\ \mathcal{P}_2 & \langle [0.35, 0.43], [0.26, 0.32], [0.13, 0.19] \rangle & \langle [0.30, 0.35], [0.25, 0.31], [0.15, 0.21] \rangle & \langle [0.37, 0.45], [0.26, 0.30], [0.14, 0.20] \rangle & \langle [0.15, 0.20], [0.18, 0.21], [0.22, 0.30] \rangle & \langle [0.14, 0.19], [0.18, 0.20], [0.21, 0.26] \rangle \\ \mathcal{P}_3 & \langle [0.18, 0.21], [0.15, 0.20], [0.10, 0.16] \rangle & \langle [0.11, 0.20], [0.13, 0.19], [0.09, 0.15] \rangle & \langle [0.15, 0.25], [0.16, 0.25], [0.12, 0.18] \rangle & \langle [0.32, 0.40], [0.34, 0.38], [0.15, 0.20] \rangle & \langle [0.30, 0.34], [0.35, 0.42], [0.11, 0.16] \rangle \\ \mathcal{P}_4 & \langle [0.25, 0.33], [0.21, 0.25], [0.12, 0.17] \rangle & \langle [0.23, 0.30], [0.24, 0.29], [0.13, 0.18] \rangle & \langle [0.24, 0.35], [0.17, 0.28], [0.14, 0.19] \rangle & \langle [0.16, 0.23], [0.20, 0.23], [0.23, 0.29] \rangle & \langle [0.16, 0.21], [0.20, 0.27], [0.25, 0.28] \rangle \end{pmatrix}.$$

- **Step 2:** These criteria of credit risk evaluation $\mathcal{O}_1, \mathcal{O}_2, \mathcal{O}_3$ belong to benefit criteria and $\mathcal{O}_4, \mathcal{O}_5$ belong to cost criteria. By using Eqs. (11) and (12), we can get:

$$\hat{\mathbf{d}}^+ = \left\{ \begin{pmatrix} \langle [0.35, 0.43], [0.15, 0.20], [0.10, 0.16] \rangle \\ \langle [0.37, 0.45], [0.16, 0.25], [0.12, 0.18] \rangle \\ \langle [0.14, 0.19], [0.35, 0.42], [0.27, 0.30] \rangle \end{pmatrix}, \begin{pmatrix} \langle [0.30, 0.35], [0.13, 0.19], [0.09, 0.15] \rangle \\ \langle [0.15, 0.20], [0.34, 0.38], [0.25, 0.32] \rangle \end{pmatrix} \right\}, \quad \hat{\mathbf{d}}^- = \left\{ \begin{pmatrix} \langle [0.18, 0.21], [0.26, 0.32], [0.13, 0.19] \rangle \\ \langle [0.15, 0.25], [0.26, 0.30], [0.14, 0.20] \rangle \\ \langle [0.30, 0.34], [0.18, 0.20], [0.11, 0.16] \rangle \end{pmatrix}, \begin{pmatrix} \langle [0.11, 0.20], [0.25, 0.31], [0.15, 0.21] \rangle \\ \langle [0.32, 0.40], [0.18, 0.21], [0.15, 0.20] \rangle \end{pmatrix} \right\}.$$

- **Step 3:** Compute the separation measures by using Eqs. (13) and (14). Using our proposed measures, we calculate the distance for risk assessment in a construction project.

$$\mathcal{V}^+ = \begin{pmatrix} & \mathcal{O}_1 & \mathcal{O}_2 & \mathcal{O}_3 & \mathcal{O}_4 & \mathcal{O}_5 \\ \mathcal{P}_1 & 0.0904 & 0.0883 & 0.1133 & 0.0791 & 0.0889 \\ \mathcal{P}_2 & 0.1510 & 0.1078 & 0.0624 & 0.1131 & 0.1349 \\ \mathcal{P}_3 & 0.1288 & 0.1289 & 0.1387 & 0.1517 & 0.1641 \\ \mathcal{P}_4 & 0.0772 & 0.0984 & 0.0744 & 0.0992 & 0.0988 \end{pmatrix},$$

$$\mathcal{V}^- = \begin{pmatrix} & \mathcal{O}_1 & \mathcal{O}_2 & \mathcal{O}_3 & \mathcal{O}_4 & \mathcal{O}_5 \\ \mathcal{P}_1 & 0.0716 & 0.0886 & 0.0591 & 0.1252 & 0.1474 \\ \mathcal{P}_2 & 0.2029 & 0.1289 & 0.1399 & 0.1433 & 0.1407 \\ \mathcal{P}_3 & 0.0897 & 0.1078 & 0.0598 & 0.1117 & 0.1300 \\ \mathcal{P}_4 & 0.0820 & 0.0922 & 0.0860 & 0.1305 & 0.1479 \end{pmatrix}.$$

- **Step 4:** Form the composite spherical fuzzy distance matrix \mathcal{V}^* based on Eq. (15).

$$\mathcal{V}^* = \begin{pmatrix} & \mathcal{O}_1 & \mathcal{O}_2 & \mathcal{O}_3 & \mathcal{O}_4 & \mathcal{O}_5 \\ \mathcal{P}_1 & -0.0188 & 0.0003 & -0.0542 & 0.0461 & 0.0585 \\ \mathcal{P}_2 & 0.0519 & 0.0211 & 0.0775 & 0.0303 & 0.0058 \\ \mathcal{P}_3 & -0.0391 & -0.0211 & -0.0790 & -0.0400 & -0.0341 \\ \mathcal{P}_4 & 0.0048 & -0.0062 & 0.0116 & 0.0313 & 0.0491 \end{pmatrix}.$$

- **Step 5:** Compute the weighted IvSFS divergence measures for each alternative according to Eq. (16). The weights assigned to each criterion are given by $w^* = (0.1919, 0.0861, 0.3464, 0.1678, 0.2078)^T$.

$$\tilde{\mathcal{V}}_1 = \sum_{j=1}^5 w_j^* \mathcal{S}_{1j}^* = -0.0025, \tilde{\mathcal{V}}_2 = \sum_{j=1}^5 w_j^* \mathcal{S}_{2j}^* = 0.0449,$$

$$\tilde{\mathcal{V}}_3 = \sum_{j=1}^5 w_j^* \mathcal{S}_{3j}^* = -0.0505, \tilde{\mathcal{V}}_4 = \sum_{j=1}^5 w_j^* \mathcal{S}_{4j}^* = 0.0199.$$

- **Step 6:** The alternatives are ranked according to their relative closeness to PIS. Based on the weighted IvSFS divergence measures of each alternative, denoted as $\tilde{\mathcal{V}}_i$, the ranking order is determined as follows: $\tilde{\mathcal{V}}_2 > \tilde{\mathcal{V}}_4 > \tilde{\mathcal{V}}_1 > \tilde{\mathcal{V}}_3$, making alternative \mathcal{P}_2 the top choice. In evaluating the risk profiles of the construction projects across the five critical criteria, it is observed that project \mathcal{P}_2 performs better in criterion \mathcal{O}_3 (Legal Issues). Since \mathcal{O}_3 has the highest weight among the evaluated criteria, this further strengthens that \mathcal{P}_2 is the most optimal choice among the alternatives. However, it is important to note that \mathbb{D}_L^2 does not conform to this ranking order and fails to accurately capture the relative proximity to the PIS, which may result in an incorrect assessment of the alternatives.

The results, shown in Table 5 and Fig. 4, reveal the ranking of alternatives to the ideal solution as follows:

- First: \mathcal{P}_2 (Commercial office construction)
- Second: \mathcal{P}_4 (Industrial warehouse construction)
- Third: \mathcal{P}_1 (Residential construction)
- Fourth: \mathcal{P}_3 (Infrastructure construction)

Based on the analysis, commercial office construction is identified as the best option for a low-risk, sustainable, and profitable construction project. It offers an ideal balance of critical criteria, making it the most suitable choice to achieve the project's safety goals, cost-effectiveness, regulatory compliance, environmental friendliness, and technical feasibility.

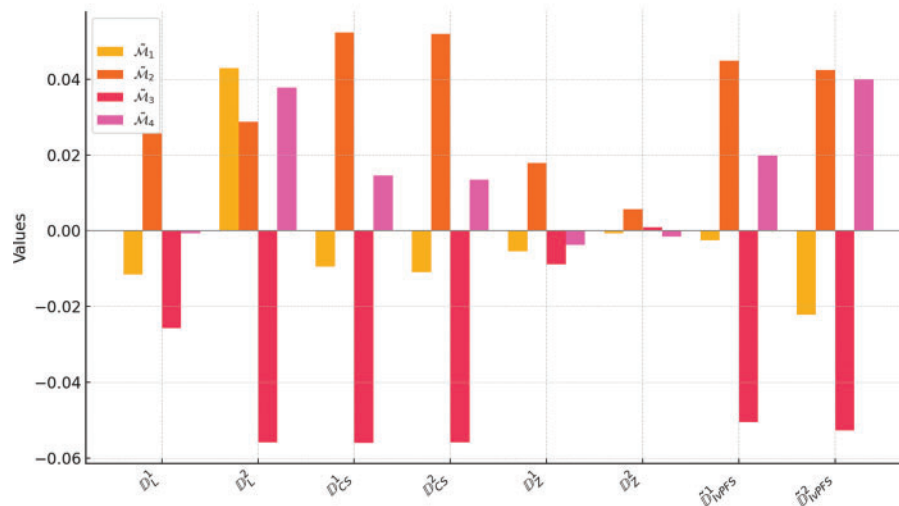
Table 5: The sustainable transport system selection results of TOPSIS

	$\tilde{\mathcal{V}}_1$	$\tilde{\mathcal{V}}_2$	$\tilde{\mathcal{V}}_3$	$\tilde{\mathcal{V}}_4$	Ranking	Best transport system
\mathbb{D}_L^1	-0.0115	0.0257	-0.0257	-0.0007	$\tilde{\mathcal{V}}_2 > \tilde{\mathcal{V}}_4 > \tilde{\mathcal{V}}_1 > \tilde{\mathcal{V}}_3$	\mathcal{P}_2
\mathbb{D}_L^2	0.0429	0.0288	-0.0559	0.0378	$\tilde{\mathcal{V}}_1 > \tilde{\mathcal{V}}_4 > \tilde{\mathcal{V}}_2 > \tilde{\mathcal{V}}_3$	\mathcal{P}_1
\mathbb{D}_{CS}^1	-0.0095	0.0524	-0.0560	0.0146	$\tilde{\mathcal{V}}_2 > \tilde{\mathcal{V}}_4 > \tilde{\mathcal{V}}_1 > \tilde{\mathcal{V}}_3$	\mathcal{P}_2
\mathbb{D}_{CS}^2	-0.0109	0.0520	-0.0559	0.0135	$\tilde{\mathcal{V}}_2 > \tilde{\mathcal{V}}_4 > \tilde{\mathcal{V}}_1 > \tilde{\mathcal{V}}_3$	\mathcal{P}_2
\mathbb{D}_Z^1	-0.0055	0.0179	-0.0088	-0.0037	$\tilde{\mathcal{V}}_2 > \tilde{\mathcal{V}}_4 > \tilde{\mathcal{V}}_1 > \tilde{\mathcal{V}}_3$	\mathcal{P}_2
\mathbb{D}_Z^2	-0.0007	0.0057	0.0009	-0.0015	$\tilde{\mathcal{V}}_2 > \tilde{\mathcal{V}}_3 > \tilde{\mathcal{V}}_1 > \tilde{\mathcal{V}}_4$	\mathcal{P}_2
$\tilde{\mathbb{D}}_{IvPFS}^1$	-0.0025	0.0449	-0.0505	0.0199	$\tilde{\mathcal{V}}_2 > \tilde{\mathcal{V}}_4 > \tilde{\mathcal{V}}_1 > \tilde{\mathcal{V}}_3$	\mathcal{P}_2

(Continued)

Table 5 (continued)

	$\tilde{\nu}_1$	$\tilde{\nu}_2$	$\tilde{\nu}_3$	$\tilde{\nu}_4$	Ranking	Best transport system
\tilde{D}_{IvPFS}^2	-0.0222	0.0425	-0.0527	0.0400	$\tilde{\nu}_2 > \tilde{\nu}_4 > \tilde{\nu}_1 > \tilde{\nu}_3$	\mathcal{P}_2

**Figure 4:** The most sustainable transport system selection result

6 Conclusion

This paper presents two divergence measures for IvPFSs by the Jensen-Shannon divergence, to overcome the limitations of existing measures. These proposed measures have completed comprehensive validation and meet all required axioms, which ensure a robust and consistent approach to measuring distance in an interval-valued fuzzy environment. The proposed divergence measures enhance accuracy and reliability in construction project risk assessment by capturing subtleties overlooked by previous methods. Its application in ranking project risks has shown promising results, supporting better decision-making for safety and efficiency in real-world scenarios. In future work, we intend to extend the proposed divergence measure to complex interval-valued picture fuzzy sets (CIvPFSs) to improve the flexibility of fuzzy sets in evaluating risks in construction projects. This extension aims to broaden its applicability, providing a more comprehensive framework for addressing uncertainties and capturing complex risk factors in construction and other critical decision-making environments. Additionally, we aim to explore the development of an improved interval-valued picture fuzzy FN-MABAC model that incorporates the proposed divergence measures. Given FN-MABAC's strong resistance to rank reversal and its ability to reflect decision-maker preferences, integrating it with our divergence framework may further improve ranking accuracy and robustness.

Acknowledgement: The authors would like to express their gratitude to King Khalid University, Saudi Arabia, for providing administrative and technical support.

Funding Statement: The authors extend their appreciation to the Deanship of Research and Graduate Studies at King Khalid University for funding this work through Small Research Project under grant number RGP1/141/46.

Author Contributions Conceptualization, Zhe Liu; methodology, Zhe Liu; software, Sijia Zhu; validation, Sijia Zhu, Yuhua Li and Akila Thiyagarajan; formal analysis, Yuhua Li, Akila Thiyagarajan and Rajanikanth Aluvalu; investigation, Sijia Zhu and Prasanalakshmi Balaji; resources, Prasanalakshmi Balaji and Zhe Liu; writing—original draft preparation, Sijia Zhu and Yuhua Li; writing—review and editing, Prasanalakshmi Balaji, Akila Thiyagarajan, Rajanikanth Aluvalu and Zhe Liu; visualization, Sijia Zhu, Yuhua Li and Rajanikanth Aluvalu; supervision, Zhe Liu; project administration, Prasanalakshmi Balaji and Akila Thiyagarajan; funding acquisition, Prasanalakshmi Balaji. All authors reviewed the results and approved the final version of the manuscript.

Availability of Data and Materials: Data information is included in this paper.

Ethics Approval: Not applicable.

Conflicts of Interest: The authors declare no conflicts of interest to report regarding the present study.

References

1. Liu Z, Letchmunan S. Enhanced fuzzy clustering for incomplete instance with evidence combination. *ACM Trans Knowl Discov Data*. 2024;18(3):1–20. doi:10.1145/3638061.
2. Liu Z. A new sine similarity measure based on evidence theory for conflict management. *Commun Stat Theory Methods*. 2025;54(11):3350–66. doi:10.1080/03610926.2024.2391415.
3. Barandas M, Famiglini L, Campagner A, Folgado D, Simão R, Cabitza F, et al. Evaluation of uncertainty quantification methods in multi-label classification: a case study with automatic diagnosis of electrocardiogram. *Inf Fusion*. 2024;101(3):101978. doi:10.1016/j.inffus.2023.101978.
4. Liu Z, Qiu H, Letchmunan S, Deveci M, Abualigah L. Multi-view evidential c-means clustering with view-weight and feature-weight learning. *Fuzzy Sets Syst*. 2025;498(12):109135. doi:10.1016/j.fss.2024.109135.
5. Alreshidi NA, Shah Z, Khan MJ. Similarity and entropy measures for circular intuitionistic fuzzy sets. *Eng Appl Artif Intell*. 2024;131(10):107786. doi:10.1016/j.engappai.2023.107786.
6. Fahmi A, Hassan MAS, Khan A, Abdeljawad T, Almutairi DK. A bipolar Fermatean fuzzy Hamacher approach to group decision-making for electric waste. *Eur J Pure Appl Math*. 2025;18(1):5691–1. doi:10.29020/nybg.ejpam.v18i1.5691.
7. Fahmi A, Khan A, Maqbool Z, Abdeljawad T. Circular intuitionistic fuzzy Hamacher aggregation operators for multi-attribute decision-making. *Sci Rep*. 2025;15(1):5618. doi:10.1038/s41598-025-88845-0.
8. Fahmi A, Khan A, Abdeljawad T, Hassan MAS, Almutairid DK. Einstein aggregation operators with cubic Fermatean fuzzy sets. *Eur J Pure Appl Math*. 2025;18(2):5891. doi:10.29020/nybg.ejpam.v18i2.5891.
9. Chu J, Xiao X. Benefits evaluation of the Northeast Passage based on grey relational degree of discrete Z-numbers. *Inf Sci*. 2023;626(4):607–25. doi:10.1016/j.ins.2023.02.085.
10. Song Y, Lin H, Li Z. Outlier detection in a multiset-valued information system based on rough set theory and granular computing. *Inf Sci*. 2024;657(1):119950. doi:10.1016/j.ins.2023.119950.
11. Cheng R, Fan J, Wu M, Seiti H. A dual-level multi-attribute group decision-making model considering interaction factors based on CCSD and MARCOS methods with R-numbers. *Expert Syst Appl*. 2024;243(20):122839. doi:10.1016/j.eswa.2023.122839.
12. Zadeh LA. Fuzzy sets. *Inf Control*. 1965;8(3):338–53. doi:10.1016/S0019-9958(65)90241-X.
13. Jebadass JR, Balasubramaniam P. Color image enhancement technique based on interval-valued intuitionistic fuzzy set. *Inf Sci*. 2024;653:119811. doi:10.1016/j.ins.2023.119811.
14. Ferreira MA, Ribeiro LC, Schuffner HS, Libório MP, Ekel PI. Fuzzy-set-based multi-attribute decision-making, its computing implementation, and applications. *Axioms*. 2024;13(3):142. doi:10.3390/axioms13030142.
15. Kizielewicz B, Sałabun W. Benchmark study of re-identification methods based on stochastic fuzzy normalization and their application to decision-making problems in engineering. *Facta Univ Ser Mech Eng*. 2025;23(1):145–60. doi:10.22190/FUME240123008K.
16. Atanassov KT. Intuitionistic fuzzy sets. *Fuzzy Sets Syst*. 1986;20(1):87–96. doi:10.1016/S0165-0114(86)80034-3.

17. Dutta D, Dutta P, Gohain B. Similarity measure on intuitionistic fuzzy sets based on Benchmark Line and its diverse applications. *Eng Appl Artif Intell.* 2024;133(2):108522. doi:10.1016/j.engappai.2024.108522.
18. Ejegwa PA, Onyeke IC, Kausar N, Kattel P. A new partial correlation coefficient technique based on intuitionistic fuzzy information and its pattern recognition application. *Int J Intell Syst.* 2023;38(1):5540085. doi:10.1155/2023/5540085.
19. Wang T, Wu X, Garg H, Liu Q. Novel strict intuitionistic fuzzy similarity measures based on fuzzy negation and their applications. *Expert Syst Appl.* 2024;252(1):124192. doi:10.1016/j.eswa.2024.124192.
20. Mahmood T, Ahmmad J, Ali Z, Yang M-S. Confidence level aggregation operators based on intuitionistic fuzzy rough sets with application in medical diagnosis. *IEEE Access.* 2023;11(12):8674–88. doi:10.3390/sym14122537.
21. Kizielewicz B, Więckowski J, Sałabun W. Fuzzy normalization-based multi-attributive border approximation area comparison. *Eng Appl Artif Intell.* 2025;141(1):109736. doi:10.1016/j.engappai.2024.109736.
22. Atanassov KT. Operators over interval valued intuitionistic fuzzy sets. *Fuzzy Sets Syst.* 1994;64(2):159–74. doi:10.1016/0165-0114(94)90331-x.
23. Malik M, Gupta SK. On basic arithmetic operations for interval-valued intuitionistic fuzzy sets using the Hamming distance with their application in decision making. *Expert Syst Appl.* 2024;239(3):122429. doi:10.1016/j.eswa.2023.122429.
24. Kalsoom U, Ullah K, Akram M, Pamucar D, Senapati T, Naeem M, et al. Schweizer-Sklar power aggregation operators based on complex interval-valued intuitionistic fuzzy information for multi-attribute decision-making. *Int J Comput Intell Syst.* 2023;16(1):170. doi:10.1007/s44196-023-00343-1.
25. Cuong BC, Kreinovich V. Picture fuzzy sets—a new concept for computational intelligence problems. In: 2013 Third World Congress on Information and Communication Technologies (WICT 2013); 2013 Dec 15–18; Hanoi, Vietnam. p. 1–6. doi:10.1109/wict.2013.7113099.
26. Luo M, Zhang G. Divergence-based distance for picture fuzzy sets and its application to multi-attribute decision-making. *Soft Comput.* 2024;28(1):253–69. doi:10.1007/s00500-023-09205-6.
27. Kahraman C. Proportional picture fuzzy sets and their AHP extension: application to waste disposal site selection. *Expert Syst Appl.* 2024;238(3):122354. doi:10.1016/j.eswa.2023.122354.
28. Singh A, Kumar S. Picture fuzzy set and quality function deployment approach based novel framework for multi-criteria group decision making method. *Eng Appl Artif Intell.* 2021;104(6):104395. doi:10.1016/j.engappai.2021.104395.
29. Devi NSK, Narayanamoorthy S, Nallasivan Parthasarathy T, Thilagasree CS, Pamucar D, Simic V, et al. An integrated bipolar picture fuzzy decision-driven system to scrutinize food waste treatment technology through assorted factor analysis. *Comput Model Eng Sci.* 2024;140(3):2665–87. doi:10.32604/cmesci.2024.029374.
30. Cuong BC, Kreinovich V. Picture fuzzy sets. *J Comput Sci Cybern.* 2014;30(4):409–20. doi:10.15625/1813-9663/30/4/5032.
31. Kishorekumar M, Karpagadevi M, Krishnaprakash S, Mariappan R, Ramesh R. Interval-valued picture fuzzy topological spaces and application of interval-valued picture fuzzy sets in multi-criteria decision-making. In: AIP Conference Proceedings. Melville, NY, USA: AIP Publishing; 2024. Vol. 3122. p. 1–6. doi:10.1063/5.0216036.
32. Zhu S, Liu Z, Ulutagay G, Deveci M, Pamučar D. Novel α -divergence measures on picture fuzzy sets and interval-valued picture fuzzy sets with diverse applications. *Eng Appl Artif Intell.* 2024;136(12):109041. doi:10.1016/j.engappai.2024.109041.
33. Amanathulla S, Khatun J. Multiple attribute decision making problem using interval-valued picture fuzzy graphs. *J Fuzzy Ext Appl.* 2025;6(2):284–99. doi:10.22105/jfea.2025.397502.1298.
34. Khan WA, Zahid A, Rashmanlou H. Novel concepts of strong paired domination in interval-valued picture fuzzy graphs and their applications towards selection criteria. *J Appl Math Comput.* 2024;1–29. doi:10.1007/s12190-024-02101-9.
35. Shanthi SA, Gayathri M. Efficiency of eco-friendly construction materials in interval-valued picture fuzzy soft environment. In: Recent developments in algebra and analysis. Cham, Switzerland: Birkhäuser; 2024. p. 245–54. doi:10.1007/978-3-031-37538-5_24.

36. Gul R, Sarfraz M. Enhancing artificial intelligence models with interval-valued picture fuzzy sets and Sugeno-Weber triangular norms. *Spectrum Eng Manag Sci.* 2025;3(1):126–46. doi:10.1234/sem.2025.0301126.
37. Khalil AM, Li S-G, Garg H, Li H, Ma S. New operations on interval-valued picture fuzzy set, interval-valued picture fuzzy soft set and their applications. *IEEE Access.* 2019;7:51236–53. doi:10.1109/access.2019.2910844.
38. Ma Q, Sun H, Chen Z, Tan Y. A novel MCDM approach for design concept evaluation based on interval-valued picture fuzzy sets. *PLoS One.* 2023;18(11):e0294596. doi:10.1371/journal.pone.0294596.
39. Ejegwa PA, Anum MT, Kausar N, Nwokoro CO, Aydin N, Yu H. New Fermatean fuzzy distance metric and its utilization in the assessment of security crises using the MCDM technique. *Math.* 2024;12(20):3214. doi:10.3390/math12203214.
40. Mishra AR, Chen S-M, Rani P. Multi-attribute decision-making based on picture fuzzy distance measure-based relative closeness coefficients and modified combined compromise solution method. *Inf Sci.* 2024;664(6):120325. doi:10.1016/j.ins.2024.120325.
41. Hatzimichailidis AG, Papakostas GA, Kaburlasos VG. A novel distance measure of intuitionistic fuzzy sets and its application to pattern recognition problems. *Int J Intell Syst.* 2012;27(4):396–409. doi:10.1002/int.21529.
42. Jiang Q, Jin X, Lee S-J, Yao S. A new similarity/distance measure between intuitionistic fuzzy sets based on the transformed isosceles triangles and its applications to pattern recognition. *Expert Syst Appl.* 2019;116(1):439–53. doi:10.1016/j.eswa.2018.08.046.
43. Wu X, Zhu Z, Chen S-M. Strict intuitionistic fuzzy distance/similarity measures based on Jensen-Shannon divergence. *Inf Sci.* 2024;661(6):120144. doi:10.1016/j.ins.2024.120144.
44. Singh P, Mishra NK, Kumar M, Saxena S, Singh V. Risk analysis of flood disaster based on similarity measures in picture fuzzy environment. *Afr Mat.* 2018;29(7–8):1019–38. doi:10.1007/s13370-018-0597-x.
45. Yuan J, Chen Z, Wu M. A novel distance measure and CRADIS method in picture fuzzy environment. *Int J Comput Intell Syst.* 2023;16(1):186. doi:10.1007/s44196-023-00354-y.
46. Zhu S, Liu Z, Ur Rahman A. Novel distance measures of picture fuzzy sets and their applications. *Arab J Sci Eng.* 2024;49(9):12975–88. doi:10.1007/s13369-024-08925-7.
47. Xu ZS, Chen J. An overview of distance and similarity measures of intuitionistic fuzzy sets. *Int J Uncertain Fuzziness Knowl Based Syst.* 2008;16(4):529–55. doi:10.1142/s0218488508005406.
48. Gohain B, Chutia R, Dutta P. A distance measure for optimistic viewpoint of the information in interval-valued intuitionistic fuzzy sets and its applications. *Eng Appl Artif Intell.* 2023;119(1):105747. doi:10.1016/j.engappai.2022.105747.
49. Mishra AR, Rani P, Pardasani KR, Mardani A, Stević Ž, Pamučar D. A novel entropy and divergence measures with multi-criteria service quality assessment using interval-valued intuitionistic fuzzy TODIM method. *Soft Comput.* 2020;24(15):11641–11661. doi:10.1007/s00500-019-04627-7.
50. Zhu S, Liu Z. Distance measures of picture fuzzy sets and interval-valued picture fuzzy sets with their applications. *AIMS Math.* 2023;8(12):29817–48. doi:10.3934/math.20231525.
51. Khan WA, Arif W, Rashmanlou H, Kosari S. Interval-valued picture fuzzy hypergraphs with application towards decision making. *J Appl Math Comput.* 2024;70(2):1103–25. doi:10.1007/s12190-024-01996-7.
52. Liu P, Munir M, Mahmood T, Ullah K. Some similarity measures for interval-valued picture fuzzy sets and their applications in decision making. *Information.* 2019;10(12):369. doi:10.3390/info10120369.
53. Cao G, Shen L. A novel parameter similarity measure between interval-valued picture fuzzy sets with its application in pattern recognition. *J Intell Fuzzy Syst.* 2023;44(6):10213–39. doi:10.3233/JIFS-224314.